A HIGH-RESOLUTION RECONSTRUCTION OF PALEO-HURRICANE STRIKES FROM THE BLUE HOLE, BELIZE

KATHRYN C. DENOMMEE

A HIGH-RESOLUTION RECONSTRUCTION OF PALEO-HURRICANE STRIKES FROM THE BLUE HOLE, BELIZE

By

© Kathryn C. Denommee

A thesis submitted to the

School of Graduate Studies

in partial fulfillment of the

requirements for the degree of

Master of Science

Department of Earth Sciences

Memorial University of Newfoundland

April 2011

St. John's Newfoundland

ABSTRACT

Annually laminated sediments are one of the most valuable sources of paleo-climatic proxy records. Sediment cores collected from the Blue Hole of Lighthouse Reef, Belize provide a continuous, high-resolution proxy record for hurricane strikes spanning the past ca. 1200 years. This record is based on the identification of anomalous graded beds, interpreted as event layers that are deposited as overwash material under the influence of tropical storms and hurricanes. These beds are found interbedded with normal background sediments that consist of annually laminated biogenic carbonate muds that, in combination with ^{14}C AMS dating, allow for the development of an absolute storm chronology. In order to facilitate the recognition and counting of these not always well-developed laminations, a new quantitative method was developed for use with the widely-used Geoscan line scanning camera system. The hurricane signal at the Blue Hole was found to exhibit multi-centennial frequency variability, with periods of increased activity occurring between ~1100 and 600 yBP and ~100 yBP to present, and a period of decreased activity occurring between ~600 and 100 yBP. These frequency shifts correspond other North Atlantic Basin paleoclimatic features, in particular sea surface temperature variations observed during the Medieval Warm Period and the Little Ice Age and known migration patterns of the Inter-tropical Convergence Zone.

ACKNOWLEDGMENTS

Firstly, I would like to thank my supervisor, Dr. Sam Bentley, for his support and guidance throughout my MSc. program. Under his supervision not only was I able to undertake this MSc. project, but I also had the opportunity travel some of the most exotic locations on the continent. Most importantly, Sam opened the world of sedimentology to me, saving me from what inevitably would have been a career spent delineating subterranean contaminant plumes. I would also like to thank Drs. Joe Macquaker (Memorial University) and Andre Droxler (Rice University) for their assistance on this project and for serving on my supervisory committee.

For their invaluable field assistance I would like to thank Drs. Sam Bentley and Andre Droxler, as well as Justin Dawe and Keegan Droxler. I would like to thank Mario Guerrero, Tony, Breeze, Poncho, and the rest of the crew from Manta Ray Charters operating out of Belize City, Belize, for providing us with phenomenal service (and freshly caught seafood) throughout the duration of the field program. I would also like to thank Drs. Scott Lamoureux (Queen's University) and Brian Menounos (University of Northern British Columbia) for generously allowing me the use of their vibracoring system to collect sediment samples from the Blue Hole. The government of Belize and the Belize Audubon Society provided the necessary permissions and permits that allowed us to conduct this scientific research. Wanda Aylward, Dario Harazim, Lina Stolze and Elisabeth Khalmeyer, and Christopher Phillips all proved to be invaluable resources in the lab.

This work was supported by funding from numerous sources including a Collaborative Research Network (CRN) Grant from the Inter-American Institute for Global Change Research (IAI) awarded to Dr. Kam-Biu Liu (Louisiana State University) and a network of 12 other researchers which includes my supervisor, Dr. Sam Bentley. Additional support was provided in the form of student research grants and awards from the Geological Society of America, the Society for Sedimentary Geology, and Memorial University.

Finally, I would like to thank my entire family for their continual support (and occasional financial contributions) but especially my mom and Dario without whom I could never have undertaken this project.

TABLE OF CONTENTS

List of Tables

Chapter 3

List of Figures

Chapter 1

Chapter 2

Chapter 3

List of appendices

CO-AUTHORSHIP STATEMENT

The following thesis chapters are presented in manuscript format. It is the intention of the authors that Chapters 2 and 3 will be submitted to peer-reviewed scientific journals. Consequently, these chapters have all been collaborative efforts between myself (the author of this thesis) and others. For each manuscript contained in this thesis I outline the work personally done and the contributions made by my co-authors. As the author of this thesis, the work is predominantly my own, with guidance from my supervisor and co-author Dr. Sam Bentley.

Chapter 2 is a methods paper that presents a quantitative technique developed to aid in the detection and counting of laminations, which are not always well developed in sediment cores collected from the Blue Hole. I preformed of the all data collection and laboratory analyses for this work. Wanda Aylward provided technical expertise, helping to operate and calibrate the MSCL. Samples for ^{14}C AMS geochronology were collected by myself with guidance from Dr. Andre Droxler (Rice University) and sent to Université Laval for sample preparation and subsequently to the University of California at Irvine for analysis. The Matlab code presented in this manuscript was compiled by David Shea, with input from myself and Dr. Samuel Bentley. I am the primary author on this manuscript with Dr. Samuel Bentley providing guidance and editorial comments. Funding for this work was provided in the form of a grant from the Inter-American Institute for

Global Change Research to Dr. Samuel Bentley with additional monies awarded to myself in the form of student research grants from the Geological Society of America and the Society for Sedimentary Geology.

Chapter 3 is a high-resolution record of hurricane strikes from the Blue Hole, Belize, reconstructed from a sediment-derived proxy. Field work to collect sediment cores consisted of a two week field season in June 2009 and was undertaken by myself, my supervisor Dr. Samuel Bentley, and Dr. Andre Droxler (Rice University) who has expert knowledge of the Belize Atoll System. All of the authors were involved in the logistics and planning of the field season. I preformed all data collection and analytical work for this project with the exception of ^{14}C AMS analyses. Samples for ^{14}C AMS geochronology were collected by myself with guidance from Dr. Andre Droxler and sent to Université Laval for sample preparation and subsequently to the University of California at Irvine for analysis. I am the primary author on this manuscript with my Drs. Samuel Bentley and Andre Droxler providing guidance and editorial comments. Funding for this work was provided in the form of a grant from the Inter-American Institute for Global Change Research to Dr. Samuel Bentley with additional monies awarded to myself in the form of student research grants from the Geological Society of America and the Society for Sedimentary Geology.

CHAPTER 1

PALEOTEMPESTOLOGY: AN INTRODUCTION AND OVERVIEW

1.1 Introduction and Overview

Tropical cyclones are the most destructive of all storms, causing more insured losses than any other natural disaster (Murnane and Liu, 2004). The combination of strong winds, flooding rains, storm surge, and tornadoes commonly causes significant loss of life, destruction of property, and dramatic geomorphic changes to coastal areas (Keim and Muller, 2007). The devastation caused by the landfall of intense tropical cyclones was brought center stage during the hurricane season of 2005, which saw an unprecedented number of named storms form in the Atlantic Basin (twenty-seven), including fifteen hurricanes, seven of which were category 3 or higher on the Saffir-Simpson scale (Trenberth and Shea, 2006; Virmani and Weisberg, 2006). These storms have always, and will always be part of the North Atlantic climate system and because coastal populations throughout the Atlantic Basin continue to grow, there is an enormous societal need to understand the potential range in the natural variability of these storms (McCloskey and Keller, 2009). By understanding better the natural variability of hurricane activity it is hoped that future losses may be minimized through better planning, more accurate forecasting, and better emergency management procedures (Murnane and Liu, 2004).

1.2 Storminess of the North Atlantic: the motivation for paleotempestology

Hurricane activity in the North Atlantic Basin is known to exhibit variability on inter-annual to millennial time scales. An examination of the historical record reveals somewhat cyclical variations in hurricane activity in the North Atlantic on the order of inter-annual to inter-decadal time scales (Goldenberg, 2001). The interannual variation in hurricane activity is relatively well understood, and has been tied to several natural phenomena including the El-Niño-Southern Oscillation (ENSO), Atlantic Basin sea level atmospheric pressure, West African monsoons, and the quasi-biennial oscillation of stratospheric wind (Chu, 2004). Of these, ENSO appears to be the most dominant factor controlling tropical cyclone activity, doing so through its effects on atmospheric conditions such as vertical wind shear, and ocean temperatures (Murnane and Liu, 2004). Scientists are able to forecast these phenomena and seasonal predictions of Atlantic Basin hurricane activity take them into account. For example, during an El Niña event, the likelihood is that the United Sates will see a greater number of hurricanes come onshore than during an El Niño event (Chu, 2004). Inter-decadal variations in hurricane activity are less well understood than interannual variations, but have also been statistically linked to naturally occurring climate phenomena. In the case of inter-decadal variations, changes in sea surface temperature in the North Atlantic and atmospheric pressure anomalies have shown the most control (Elsner et al., 1999; Goldenberg et al., 2001; Landsea et al., 1999). These inter-decadal variations are known to affect not only the temporal distribution of major hurricanes, but also their spatial distribution (Goldenberg et al., 2001).

The historical record does not extend back far enough to offer any real insight as to how hurricane activity may vary on timescales beyond decadal. Fortunately, geological proxies have the potential to extend the hurricane record by centuries to millennia. In exploiting these geological archives, scientists are better able to understand how long-term shifts in climatic phenomena may influence hurricane activity.

1.3 Paleotempestology: the sedimentary record as a tropical cyclone archive

The inability of scientists to identify long-term patterns in hurricane activity due to the brief nature of both the historical and meteorological records for the North Atlantic Basin is being overcome in part by paleotempestology - the reconstruction of the paleohurricane record through the use of and geological and biological proxy methods (Frappier et al., 2007; Liu, 2004b, 2007). The anticipated application of this science is to be able to provide better statistical constraints on hurricane prediction, and to understand better how climate change may influence the formation and trajectories of catastrophic hurricanes in the future (Hippensteel, 2008). Unfortunately, this field of study does not in itself have the potential to provide a good estimate of the future probability of extreme hurricane events (Frappier et al., 2007). This is because there are no good analogs for both anticipated climate warming and associated storm impacts to be found in the geological record (Frappier et al., 2007). It does however, have the potential to provide new insights into how large-scale atmospheric forcing mechanisms influence hurricane formation and trajectories by correlating paleohurricane proxy records with paleoclimatic proxy records.

At its inception, paleotempestology focused on recreating the hurricane record from overwash sediments that are transported landward and deposited in back-barrier settings by storm surge and waves (Liu and Fearn, 1993). These hurricane-generated deposits form event layers that are distinguished from their host sediments on the basis of lithological and sedimentological evidence and are subsequently dated using standard radiometric techniques including $^{210}Pb/^{137}Cs$ for younger events, and ^{14}C for older events. The records established from these back-barrier sedimentary records provide a "worst case scenario" estimate of hurricane activity (Frappier et al., 2007). They are more likely to identify catastrophic events, those measuring as Category 3 or higher on the Saffir-Simpson scale which have long return periods (> 100s of years), than they are to preserve a complete record of paleohurricane activity including less extreme storms. More recently however, an increase in the use of high-resolution paleotempestological proxies (such as the one presented in Chapter 3 of this thesis) has generated a series of annually resolved hurricane records for several locations in the North Atlantic Basin that have the potential to preserve a more comprehensive hurricane record. Unfortunately the high-resolution records established to date are much shorter than their low-resolution counterparts, covering at most the past ~1500 years (Besonen et al., 2008; Denommee and Bentley, 2010; Donnelly et al., 2001).

In order to fully exploit these unique archives and gain a better understanding of paleohurricane activity in the North Atlantic Basin, it is necessary to expand the spatial coverage of paleotempestological study sites. Ideally these new reconstructions will yield high-resolution records spanning several millennia which would allow for more meaningful comparisons between study locations and the development of a better understanding of how hurricanes have behaved in the past and the implications for future storm activities.

1.4 The Bermuda High Hypothesis: expanding the spatial coverage of paleotempestological records for the Caribbean

Paleotempestological reconstructions throughout the North Atlantic Basin show evidence of long term variability in the activity regimes of hurricanes (Besonen et al., 2008; Donnelly, 2005; Donnelly and Webb, 2004; Knowles, 2008; Liu, 1999, 2004b; Liu and Fearn, 1993, 1997; Liu, 2000; Mann et al., 2009; McCloskey, 2009; McCloskey and Keller, 2009; Scott et al., 2003, 2005). More strikingly, there is a widespread recognition of the existence of abrupt shifts in the landfalling hurricane activity throughout the North Atlantic Basin (McCloskey, 2009). The recognition of these abrupt shifts has led to the formulation of two models, each of which attempts to explain possible mechanisms for the observed shifts between active and quiet periods of landfalling hurricane activity.

One model put forth by Donnelly and Woodruff (2007) attributes the shift between active and quiet periods of landfalling hurricane activity to synchronous changes in basin-wide climatic conditions. They found that periods of increased hurricane landfalls over the past 2500 years observed in sediment-derived records from Long Island, New York (Scileppi and Donnelly, 2007) correspond to periods of increased hurricane landfalls at Vieques, Puerto Rico (Donnelly and Woodruff, 2007). Additionally, they found that a quiescent period lasting from ~1000 to 250 yBP observed at both sites, corresponds to a quiescent period observed in sediment-derived records from the Gulf of Mexico (Liu and Fearn, 2000). Donnelly and Woodruff (2007) have attributed these shifts in activity regimes to basin-wide changes in the climatic conditions that influence the formation of hurricanes. More specifically, they observed that during the late Holocene, the more active periods of landfalling hurricane activity correspond to periods with relatively few El Niño events, while more quiescent periods of landfalling hurricane activity generally correspond to periods with more frequent and strong El Niño events. They also observed that there is a strong correlation between convective storminess in tropical West Africa and hurricane frequency in the North Atlantic Basin. Periods that are characterised by increased precipitation in tropical West Africa correspond to periods of increased landfalling hurricane activity throughout the North Atlantic Basin, while the converse holds true for more periods characterized as having less convective storminess in tropical West Africa (Donnelly and Woodruff, 2007).

The second model, termed the "Bermuda High Hypothesis" (Elsner et al., 2000; Liu, 2007), interprets the observed shifts in landfalling hurricane frequencies as being the result of the time-transgressive movement of a landfalling hurricane belt. This hypothesis is based on the idea that hurricanes are an intrinsic part of the North Atlantic climate circulation system, and there has been large scale movement of this system throughout the Holocene resulting in the latitudinal migration of the hurricane zone (McCloskey, 2009). This hypothesis calls on a shift in the position of the Bermuda High – a high pressure system located in the subtropical Atlantic Ocean that steers hurricanes formed over waters near the coast of West Africa toward North America (Liu, 2007). Liu (2004b, 2007) has hypothesized that a southward migration of this system would result in more hurricanes being directed towards the Gulf Coast, while a northward migration of the systems would direct storms towards the Eastern Seaboard of the United States (Fig. 1.1). If indeed the large-scale latitudinal migration of such a climate system were controlling hurricane trajectories and subsequent landfall frequencies, there should be an anti-phase relationship between activity regimes for locations in the Caribbean/Gulf of Mexico and those along the U.S. Atlantic Coast (Elsner et al., 2000). Liu (2004b) presents a preliminary comparison of records from the U.S. Gulf and Atlantic coasts which appear to support the Bermuda High Hypothesis.

Presently, there is insufficient spatial coverage to properly resolve this debate. In particular, the pan-Caribbean region is vastly underrepresented in North Atlantic Basin paleotempestological studies (Knowles, 2008). This region is among the most hurricane-prone in the world, and developing a better understanding of paleohurricane activity in the pan-Caribbean will help us to develop a better understanding of the atmospheric forcing mechanisms that control the shifts between active and quiet periods of landfalling hurricane activity. Extending the spatial coverage of paleotempestological investigations

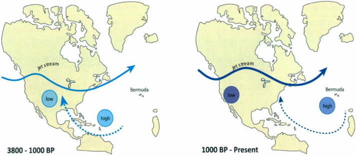

Fig. 1.1. Changes in the position of the Bermuda High high pressure system are hypothesized to account for changes in hurricane activity over time. Presently, the Bermuda High directs storms towards the East Coast of the United States (right). Between 3,400 and 1,000 yr. B.P. however, it may have been positioned more to the southwest, causing an increase in hurricane strikes along the Gulf Coast of the United Sates (left) (modified from Liu, 2007).

will also help to overcome the debate as to whether hurricane activity in the North Atlantic Basin fluctuates in a basin-wide or time-transgressive manner (McCloskey, 2009).

As part of the collaborative effort to understand the paleotempestology of the Caribbean region (Liu, 2004a), this MSc. thesis project presents a proxy record using sediments from the Blue Hole of Lighthouse Reef, Belize (Fig. 1.2). This project will "employ the principles and methods of paleotempestology with the ultimate goal of analyzing basin-wide patterns of paleohurricane activity in the context of other large-scale climate phenomena (i.e., El Niño Southern Oscillation, North Atlantic Oscillation, Atlantic sea surface temperature, and the intra-Americas low level jet)" (Liu, 2004a). In addition to advancing our understanding of the mechanisms controlling hurricane activity in the Caribbean region, the results of this study will have practical applications in the areas of hurricane risk assessment, vulnerability reduction, and disaster management policy and planning for the Caribbean region (Liu, 2004a).

1.5 Thesis Structure and Outline

This thesis is presented in manuscript format and is structured as follows: **Chapter 1**, to which this brief outline belongs, is entitled *Paleotempestology: An Introduction and Overview*. This chapter presents the motivation and scientific basis for sediment-derived proxy records of paleo-hurricane strikes, and briefly discusses their potential applications in modern climatology and hurricane risk assessment. The body of this thesis is

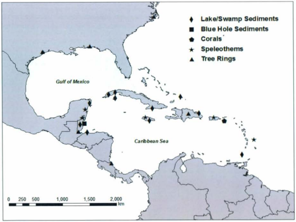

Fig. 1.2. Locations of study sites in the pan-Caribbean region included in the multi-proxy, multi-site paleotempestological study (Liu, 2004a)

contained in Chapters 2 and 3. These chapters are scientific manuscripts intended for publication in peer-reviewed journals, and are the major products of this MSc. research project. **Chapter 2** is entitled *A Simple Method for Semi-Automated Laminae Detection and Counting for use with the Geoscan Line Scan Camera System with an Example from the Blue Hole, Belize.* This chapter describes a simple, yet highly effective, method developed to aid in the detection, measurement, and counting of fine laminae that are not always well defined in the stratigraphic record – such as those observed in sediments from the Great Blue Hole, Belize. The primary motivation for this chapter was to develop an objective and quantifiable method for paleohurricane reconstruction which is the main goal of this MSc. project. **Chapter 3** is entitled *A High-Resolution Reconstruction of Paleo-hurricane Strikes from the Blue Hole, Belize.* This chapter is the primary manuscript for this MSc. project, and presents the results of a sediment-derived proxy record for hurricane strikes at the Blue Hole, Belize. The chronology of these strikes is then put into context by comparing it to other sediment-derived records from sites throughout the North Atlantic Basin as well as known climatic phenomena including the migration of the ITCZ, the LIA, the MWP, and SST records. The final chapter, **Chapter 4** is entitled *High-Resolution Paleo-hurricane Reconstructions from the Blue Hole: A Unique Contribution to the Paleotempestological Record of the Caribbean.* This chapter synthesises Chapters 2 and 3 and briefly presents the main conclusions of this MSc. thesis. Appendices which provide supplemental data and information that support the conclusions of this MSc. project are found following Chapter 4.

References

Besonen, M.R., Bradley, R.S., Mudelsee, M., Abbott, M.B., and Francus, P., 2008, A 1,000-year, annually-resolved record of hurricane activity from Boston, Massachusetts: Geophysical Research Letters, v. 35.

Chu, P.S., 2004, ENSO and tropical cyclone activity *in* Murnane, R., and Liu, K.B., eds., Hurricanes and Typhoons: Past, Present, and Future: New York, Columbia University Press.

Denommee, K., and Bentley, S., 2010, High-resolution record of cyclone strikes from the Blue Hole, Lighthouse Reef, Belize, Association of American Geographers Annual Meeting: Washington, D.C.

Donnelly, J.P., 2005, Evidence of past intense tropical cyclones from backbarrier salt pond sediments: A case study from Isla de Culebrita, Puerto Rico, USA: Journal of Coastal Research, p. 201-210.

Donnelly, J.P., Roll, S., Wengren, M., Butler, J., Lederer, R., and Webb, T., 2001, Sedimentary evidence of intense hurricane strikes from New Jersey: Geology, v. 29, p. 615-618.

Donnelly, J.P., and Webb, T., 2004, Back-barrier sedimentary records of intense hurricane landfalls in the Northeastern United Sates, *in* Murnane, R.a.L., K.B., ed., Hurricanes and Typhoons: Past, Present and Future: New York, Columbia University Press.

Donnelly, J.P., and Woodruff, J.D., 2007, Intense hurricane activity over the past 5,000 years controlled by El Nino and the West African monsoon: Nature, v. 447, p. 465-468.

Elsner, J.B., Kara, A.B., and Owens, M.A., 1999, Fluctuations in North Atlantic hurricane frequency: Journal of Climate, v. 12, p. 427-437.

Elsner, J.B., Liu, K.B., and Kocher, B., 2000, Spatial variations in major US hurricane activity: Statistics and a physical mechanism: Journal of Climate, v. 13, p. 2293-2305.

Frappier, A., Knutson, T., Liu, K.B., and Emanuel, K., 2007, Perspective: coordinating paleoclimate research on tropical cyclones with hurricane-climate theory and modelling: Tellus Series a-Dynamic Meteorology and Oceanography, v. 59, p. 529-537.

Goldenberg, S.B., 2001, The recent increase in Atlantic hurricane activity: Causes and implications (vol 293, pg 474, 2001): Science, v. 293, p. 1997-1997.

Goldenberg, S.B., Landsea, C.W., Mestas-Nunez, A.M., and Gray, W.M., 2001, The recent increase in Atlantic hurricane activity: Causes and implications: Science, v. 293, p. 474-479.

Hippensteel, S.P., 2008, Preservation potential of storm deposits in south carolina back-barrier marshes: Journal of Coastal Research, p. 594-601.

Keim, B.D., and Muller, R.A., 2007, Spatiotemporal patterns and return periods of tropical storm and hurricane strikes from Texas to Maine: Journal of Climate, v. 20, p. 3498-3509.

Knowles, J.T., 2008, A 5000 year history of Caribbean environmental change and hurricane activity reconstructed from coastal lake sediments of the West Indies: Baton Rouge, Louisiana State University.

Landsea, C.W., Pielke, R.A., Mestas-Nunez, A., and Knaff, J.A., 1999, Atlantic basin hurricanes: Indices of climatic changes: Climatic Change, v. 42, p. 89-129.

Liu, K.B., 1999, Millenial-scale variability in catastrophic hurricane landfalls along the Gulf of Mexico coast.: Preprints of the 23rd Conference on Hurricanes and Tropical Meteorology, p. 374-377.

—, 2004a, Paleotempestology of the Caribbean Region: A Multi-proxy, Multi-site Study of the Spatial and Temporal Variability of Caribbean Hurricane Activity, Inter-American Institute for Global Change Research.

—, 2004b, Paleotempestology: Principles, methods, and examples from Gulf Coast lake sediments, *in* Murnane, R., and Liu, K.B., eds., Hurricanes and Typhoons: Past, Present and Future: New York, Columbia Press, p. 464.

—, 2007, Uncovering prehistoric hurricane activity - Examination of the geological record reveals some surprising long-term trends: American Scientist, v. 95, p. 126-133.

Liu, K.B., and Fearn, M.L., 1993, Lake-sediment record of late holocene hurricane activities from coastal Alabama: Geology, v. 21, p. 793-796.

—, 1997, Lake sediment records of hurricane opal and prehistoric hurricanes from the Florida panhandle: 22nd Conference on Hurricanes and Tropical Meteorology, p. 397-398

—, 2000, Reconstruction of prehistoric landfall frequencies of catastrophic hurricanes in northwestern Florida from lake sediment records: Quaternary Research, v. 54, p. 238-245.

Liu, K.B.M.L.F., 2000, Holocene history of catastrophic hurricane landfalls along the Gulf of Mexico coast reconstructed from coastal lake and marsh sediments, *in* Ning, Z.H.a.A., K.K. , ed., Current Stresses and Potential Vulnerabilities: Implications of Global Change for the Gulf Coast Region of the United States: Baton Rouge, Franklin Press, p. 38-47.

Mann, M.E., Woodruff, J.D., Donnelly, J.P., and Zhang, Z.H., 2009, Atlantic hurricanes and climate over the past 1,500 years: Nature, v. 460, p. 880-U115.

McCloskey, T.A., 2009, Proxy Records of Paleohurricanes for the Western and Southern Caribbean: Baton Rouge, Louisiana State University.

McCloskey, T.A., and Keller, G., 2009, 5000 year sedimentary record of hurricane strikes on the central coast of Belize: Quaternary International, v. 195, p. 53-68.

Murnane, R.J., and Liu, K.-b., 2004, Hurricanes and typhoons : past, present, and future: New York, Columbia University Press, 462 p.

Scileppi, E., and Donnelly, J.P., 2007, Sedimentary evidence of hurricane strikes in western Long Island, New York: Geochemistry Geophysics Geosystems, v. 8.

Scott, D.B., Collins, E.S., Gayes, P.T., and Wright, E., 2003, Records of prehistoric hurricanes on the South Carolina coast based on micropaleontological and sedimentological evidence, with comparison to other Atlantic Coast records: Geological Society of America Bulletin, v. 115, p. 1027-1039.

—, 2005, Records of prehistoric hurricanes on the South Carolina coast based on micropaleontological and sedimentological evidence, with comparison to other Atlantic Coast records: Discussion - Reply: Geological Society of America Bulletin, v. 117, p. 254-256.

Trenberth, K.E., and Shea, D.J., 2006, Atlantic hurricanes and natural variability in 2005: Geophysical Research Letters, v. 33.

Virmani, J.I., and Weisberg, R.H., 2006, The 2005 hurricane season: An echo of the past or a harbinger of the future?: Geophysical Research Letters, v. 33.

CHAPTER 2

A SIMPLE METHOD FOR AUTOMATED LAMINAE COUNTING AND EVENT BED DETECTION FOR USE WITH THE GEOSCAN COLOUR LINE SCAN CAMERA SYSTEM WITH AN EXAMPLE FROM THE BLUE HOLE, BELIZE

Kathryn C. Denommee[1], Samuel J. Bentley[2], and David Shea[3]

[1]*Memorial University of Newfoundland, Department of Earth Sciences, St. John's, NL, A1B 3X5*

[2]*Louisiana State University, Department of Geology and Geophysics, Baton Rouge, LA, 70803*

[3]*Memorial University of Newfoundland, Department of Ocean Engineering and Naval Architecture, St. John's, NL, A1B 3X5*

Abstract

In this paper we present a simple method for counting laminae and obtaining lamina/bed thickness measurements from high-resolution, spatially referenced digital images obtained using the Geoscan image acquisition system in combination with Geotek's ImageTools image acquisition software and a simple Matlab program. The lamina counts and thickness measurements objectively determined using this method are essential for paleoclimatic studies involving laminated sediments, and can be used to construct a chronology or to compile a time-series of laminae-thicknesses which can then be used to identify anomalous beds. Following this method, a high-resolution record of greyscale

luminance values was extracted from digital images of annually laminated sediments from the Blue Hole, Belize. The laminae-count age model was calibrated with AMS radiocarbon ages. A correlation coefficient of 0.99 between the laminae-count model and ten ^{14}C AMS ages demonstrates the validity of this method.

2.1 Introduction

Annually-laminated sediments represent excellent paleoclimatic archives (Hughen et al., 2004). Among established geological proxies, they are recognized as having the highest potential to yield detailed climate information (Schaaf and Thurow, 1997). Not only do they have the potential to provide an absolute chronology for sedimentation and depositional events but they are also a potential record of longer-term climate variability (Weber et al., 2010). Obtaining long records from these sediments can be challenging. Laminae are often thin and not well defined, making it difficult to count them and take thickness measurements. Traditionally these tasks have been preformed manually, by analysis of thin sections, or by manually investigating scanned pictures (Dean et al., 2002). These techniques, although well-established have the disadvantages of being both tedious and subjective (Rupf and Radons, 2004).

For these reasons, several efforts have been made to automate laminae recognition and counting from sediment cores (Francus et al., 2002; Meyer et al., 2006; Schaaf and Thurow, 1997; Weber et al., 2010). Among these contributions, none so far have directly published the numerical tools used for image analysis. Neither have these methods been optimized for use with the now widely available Geoscan line scanning camera system, which is part of the Geotek multi-sensor core logging system (MSCL), wherein image data can be easily manipulated and extracted with the ImageTools image analysis software supplied by Geotek. In this paper we present a simple method, along with the necessary Matlab code for the semi-automated extraction of bed or lamina thickness measurements and contact depths from high-resolution, spatially-referenced digital images captured using the afore mentioned core-logging equipment.

2.2 Methods

2.2.1 Materials

Sediment cores retrieved from the bottom of the Belize Blue Hole consist primarily of undisturbed annually laminated biogenic carbonate muds and silts which represent normal background sedimentation (Fig. 2.1). Individual laminae are observed to have thicknesses ranging from 1 to 1.5 mm and consist of alternating light (buff) and dark (green) couplets. These couplets have previously been interpreted as being annual layers, or varves, and represent seasonal fluctuations in organic productivity in the surface waters of the Lighthouse Reef lagoon (Gischler et al., 2008). Found inter-bedded with the normal background sediments are coarse-grained layers consisting of skeletal debris and detritus that range in thickness from several mm to tens of cm. They are distinguished from the normal background sediments based on colour and layer thickness > 3mm (Chapter 3). These coarse-grained layers have been interpreted as being event beds deposited as sediment overwash from hurricanes and tropical storms (Chapter 3, Gischler et al., 2008).

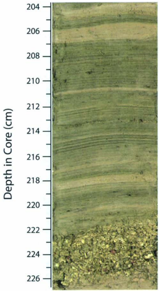

Fig. 2.1. An example of a sediment surface from the Blue Hole, Belize. The sediment consists of alternating light and dark finely laminated muds and silts that represent normal background sedimentation. The colour variations represent seasonal alterations in organic matter within the water column. During the winter months the concentration of organic matter in the water column is greater that during the summer months due to seasonal upwelling of nutrient-rich deep waters. These fine-grained laminations are interrupted by thicker coarse-grained layers which are event beds deposited by tropical cyclones in the area.

This data set represents a potentially significant and unique climate archive that has preserved not only records of Holocene climate fluctuations, but also a nearly pristine record of hurricane activity in the area based on the interpretation that the anomalous graded beds within the laminated muds represent event layers.

Determining the chronology of these sediments by manual counting of annual layers proves to be difficult because the contacts separating the laminations are not always well developed. To aid in this process a simple method was designed to be used with high-resolution colour data collected using a Geoscan line-scanning camera integrated into the Geotek MSCL, a system that is widely available in sediment core analysis laboratories.

2.2.2 *Sediment Surface Preparation*

Prior to imaging split cores, the soft-sediment core surface was scraped smooth with a metal blade. This was done in order to expose fresh sediment colour and to eliminate any surface irregularities that might produce shadows or reflect light and result in artefacts appearing in the digital images (Nederbragt and Thurow, 2005).

2.2.3 *High-Resolution Digital Imaging*

Split cores were imaged using a Geoscan colour line scan camera system integrated into a Geotek multi-sensor core logger (MSCL). The system consists a 3-CCD line scanning camera with pixel arrays of 3 x 1024 pixels mounted in a fixed position above the MSCL track. Colour filters are applied to each CCD so that there is almost complete colour separation of the data into the red, green, and blue (RGB) wavelengths and each CCD collects data from only one of these. This true colour separation allows for rigorous colour analysis to be performed on the data collected (Jorry et al., 2008; Nederbragt et al., 2004). Split cores are pushed along the track by a stepper motor that triggers the line acquisition of the camera. Since the motor pulses correspond to fixed lengths of track movement, the resulting images have precise spatial references.

2.2.4 *Image Processing*

Following the RGB image capture, Geotek ImageTools image analysis software was used to extract a horizontally averaged (20 pixels wide) RGB colour data time-series along the stratigraphic axis of the core image at 0.1 mm (1 pixel) depth intervals. This resolution can easily be altered in ImageTools depending on the material and the user's preferences. This method of extracting colour data provides users with a high degree of control, allowing user selection of the exact core interval to be measured. RGB data is collected along a relatively wide strip, as opposed to a vertical line of one pixel, because digital cameras commonly record image noise, even when objects are homogenously coloured. By collecting data along a wider vertical strip, scatter (noise) in the data is minimized because it is horizontally averaged (Nederbragt and Thurow, 2005).

The aperture-calibrated RGB time-series data is then converted to a greyscale/luminance (L*) time-series using the following equations:

$$(Rcal, Gcal, or Bcal) = (Rraw, Graw, or Braw) \times (IA^2/CA^2) \qquad \text{Eq. 1}$$

where: IA is the aperture setting used for core image capture, and

CA is the aperture setting used for light and dark field calibration

$$L^* = 0.30Rcal + 0.59Gcal + 0.11Bcal \qquad \text{Eq. 2}$$

where: L* is calibrated greyscale/luminance. (Rasband and Ferreira, 2010)

2.2.5 Automated Lamina Detection and Thickness Measurements

In the case of laminated core material, layer boundaries correspond to the inflection points of the greyscale luminance curves. Our method, like other established laminae detection methods uses a differential filter for edge detection (Cooper, 1998). In terms of core material, the filter determines the depth-referenced contact between light and dark laminae. To implement the filter, a simple Matlab program inflection.m was compiled (Appendix A) that determines a laminae count, core depth of contacts, and individual bed/lamina thicknesses.

It is important that disturbed sediment core intervals, such as the massive event-generated beds that are visible in the sediment cores from the Blue Hole are not considered in the final lamina count. These intervals are part of the real sediment thickness but may contain features that create artefacts, such as mottling or large grains, which may be recorded erroneously as bed contacts, owing to associated colour or shade changes in sediment (Fig. 2.1). The exclusion of these intervals can be done either prior to, or after running the bed-detection program. In the case of sediment cores from the Blue Hole, the disturbed intervals were excluded after running the program.

2.3 Results

The initial outputs of the Matlab program inflection.m (Appendix A) are presented as Figure 2.2 and include a time series of laminae and bed contact depths (the depth values that correspond to zero crossings of the first derivative of the lightness values) and the depth referenced lamina and bed thicknesses.

2.4 Discussion and Conclusions

The validity of this semi-automated method was tested by comparing the age model (chronology) of the sediment core materials from the Blue Hole as determined by the lamina count output from the inflection.m program to an age model constructed from ten ^{14}C AMS ages for the same sediment core materials (Chapter 3). This comparison is presented as Figure 2.3, which shows that there is a 99% correlation between the two age models.

The method presented here, like previously established methods found in the literature such as that of Nederbraght and Thurow (2001) uses generated greyscale luminance profiles to detect the contact between and count laminae. Our approach however, makes explicit use of the widely available Geoscan line-scanning camera

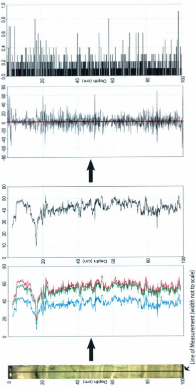

Bed Thickness (cm)
Zero Pass of 1st Derivative
Greyscale Brightness
RGBcal Brightness
Depth (cm)
Line of Measurement (width not to scale)

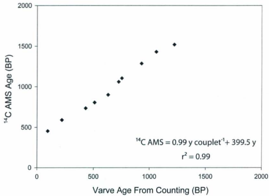

Fig. 2.3. Plot of calibrated ^{14}C AMS ages (BP) for 10 samples from the Blue Hole, Lighthouse Reef, Belize vs. the varve ages obtained from corresponding depths using the method described in this paper. Product moment correlation coefficient r = 0.99. There is an offset between the two, but the offset is thought to be the result of unaccounted older carbon entering the system (there is no ΔR value established to correct for the reservoir effect at this site) and not does not represent a hiatus in sedimentation.

system, which can be integrated into a Geotek multi-sensor core logging system (MSCL) along with ImageTools image analysis software (supplied by Geotek). Additionally we directly provide users with a simple and easy to use Matlab program to extract spatially-referenced quantitative data from these greyscale luminance profiles. In doing so, this method takes advantage of easily obtained spatially-referenced quantitative sediment colour data to provide a much more objective lamina count for finely laminated materials with poorly developed contacts that is possible through visual counting alone. Although the inability of this technique to automatically recognize mottled units limits its application, it does an excellent job of counting and measuring laminations in undisturbed sediment core material.

References

Cooper, M.C., 1998, The use of digital image analysis in the study of laminated sediments: Journal of Paleolimnology, v. 19, p. 33-40.

Dean, W., Anderson, R., Bradbury, J.P., and Anderson, D., 2002, A 1500-year record of climatic and environmental change in Elk Lake, Minnesota - I: Varve thickness and gray-scale density: Journal of Paleolimnology, v. 27, p. 287-299.

Francus, P., Keimig, F., and Besonen, M., 2002, An algorithm to aid varve counting and measurement from thin-sections: Journal of Paleolimnology, v. 28, p. 283-286.

Gischler, E., Shinn, E.A., Oschmann, W., Fiebig, J., and Buster, N.A., 2008, A 1500-Year Holocene Caribbean Climate Archive from the Blue Hole, Lighthouse Reef, Belize: Journal of Coastal Research, v. 24, p. 1495-1505.

Hughen, K., Lehman, S., Southon, J., Overpeck, J., Marchal, O., Herring, C., and Turnbull, J., 2004, C-14 activity and global carbon cycle changes over the past 50,000 years: Science, v. 303, p. 202-207.

Jorry, S.J., Droxler, A.W., Mallarino, G., Dickens, G.R., Bentley, S.J., Beaufort, L., Peterson, L.C., and Opdyke, B.N., 2008, Bundled turbidite deposition in the central Pandora Trough (Gulf of Papua) since Last Glacial Maximum: Linking sediment nature and accumulation to sea level fluctuations at millennial timescale: Journal of Geophysical Research-Earth Surface, v. 113.

Meyer, M.C., Faber, R., and Spotl, C., 2006, The WinGeol Lamination Tool: new software for rapid, semi-automated analysis of laminated climate archives: Holocene, v. 16, p. 753-761.

Nederbragt, A., and Thurow, J., 2005, Digital Sediment Colour Analysis as a Method to Obtain High Resolution Climate Proxy Records, *in* Francus, P., ed., Image Analysis, Sediments and Paleoenvironments, Volume 7: Developments in Paleoenvironmental Research, Springer Netherlands, p. 105-124.

Nederbragt, A.J., Thurow, J., Vonhof, H., and Brumsack, H.J., 2004, Modelling oceanic carbon and phosphorus fluxes: implications for the cause of the late Cenomanian Oceanic Anoxic Event (OAE2): Journal of the Geological Society, v. 161, p. 721-728.

Rasband, W., and Ferreira, T.A., 2010, Image J USA, National Institues of Health.

Rupf, I., and Radons, G., 2004, New approaches for automated data processing of annually laminated sediments: Nonlinear Processes in Geophysics, v. 11, p. 599-607.

Schaaf, M., and Thurow, J., 1997, Tracing short cycles in long records: The study of inter-annual to inter-centennial climate change from long sediment records, examples from the Santa Barbara Basin: Journal of the Geological Society, v. 154, p. 613-622.

Weber, M.E., Reichelt, L., Kuhn, G., Pfeiffer, M., Korff, B., Thurow, J., and Ricken, W., 2010, BMPix and PEAK tools: New methods for automated laminae recognition and counting-Application to glacial varves from Antarctic marine sediment: Geochemistry Geophysics Geosystems, v. 11.

CHAPTER 3

A HIGH-RESOLUTION RECONSTRUCTION OF PALEO-HURRICANE STRIKES FROM THE BLUE HOLE, BELIZE

Kathryn C. Denommee[1], Samuel J. Bentley[2], and Andre W. Droxler[3]

[1]*Memorial University of Newfoundland, Department of Earth Sciences, St. John's, NL, A1B 3X5*

[2]*Louisiana State University, Department of Geology and Geophysics, Baton Rouge, LA, 70803*

[3]*Rice University, Department of Earth Science, Houston, TX, 77251-1892*

Abstract

Sediment cores collected from the Blue Hole of Lighthouse Reef, Belize provide a continuous, high-resolution proxy record for hurricane strikes spanning the past ca. 1200 years. This record is based on the identification of background sediment patterns, as well as anomalous graded beds, interpreted as event layers deposited as overwash material under the influence of tropical storms and hurricanes. Event beds are found interbedded with normal background annually laminated biogenic carbonate muds. The hurricane signal at the Blue Hole shows multi-century frequency variability, with periods of increased activity occurring between ~1100 and 600 yBP, and from ~100 yBP to present,

and a period of decreased activity occurring between ~600 and 100 yBP. The timings of these frequency shifts correspond known paleoclimatic phenomena from the North Atlantic Basin, in particular sea surface temperature variations during the Medieval Warm Period the Little Ice Age and the long-term southerly displacement (migration) of the Inter-tropical Convergence Zone.

3.1 Introduction

The coast of Belize, like much of the North Atlantic Basin is, and has been throughout recorded history, highly vulnerable to landfalling hurricane strikes (Neumann, 1993). Since 1889, 53 tropical storms and hurricanes have been recorded making landfall or having impacts on this Central American country, including several catastrophic storms such as the unnamed storm of 1931 that destroyed two thirds of the buildings in Belize City and killed more than 2500 people (BNMS, 2010). It is clear that these storms have the potential to devastate this vulnerable region, both in terms of potential loss of life and economic impacts, consequently it is important that we better understand the long-term patterns of hurricane activity and what climatic conditions may act as forcing agents.

The observational record alone is insufficient to detect long-term (centennial to millennial) patterns in hurricane variability. However, geological proxy methods, more specifically the identification and radiometric dating of hurricane event layers preserved in the sedimentary record, have the potential to reliably extend the hurricane record and thus offer real insight into the long term behavior of North Atlantic storms (Donnelly and

Woodruff, 2007; Liu and Fearn, 2000). This approach, first described by K.O. Emery in his book *A Coastal Pond Studied by Oceanographic Methods*, is based on the observation that hurricanes can generate storm surges that crest geomorphological barriers such as dunes or barrier reefs, and deposit overwash fans which become interbedded with normal background sediments (Emery, 1969). This method for reconstructing site-specific hurricane records has been employed with varying degrees of success along the U.S. Gulf and Atlantic coastlines (Collins et al., 1999; Donnelly et al., 2001b; Donnelly and Webb, 2004; Fan and Liu, 2008; Liu and Fearn, 2000; Madsen et al., 2009; Scott et al., 2003), and to a lesser extent throughout the Caribbean (Donnelly, 2005; Donnelly and Woodruff, 2007; McCloskey, 2009; McCloskey and Keller, 2009). The results from these investigations indicate that there are centennial- to millennial-scale variations in hurricane landfalls throughout the North Atlantic Basin.

The recognition of these variations has led to the development of the "Bermuda High Hypothesis" - the hypothesis that long-term migrations of atmospheric pressure systems such as the Inter-tropical Convergence Zone (ITCZ) and the Bermuda High high pressure system (BH) could cause a migration in long-term (centennial to millennial scale) shifts in the dominant trajectory of hurricanes and their subsequent landfalling locations (Murnane and Liu, 2004). Unfortunately due to the uncertainties associated with many of these reconstructions (low resolution, uncertain chronological control, and variations in the sensitivity of sites to hurricane landfalling events) scientists have been unable to reliably discern patterns in hurricane landfall frequencies that are consistent with this (or any other) hypothesis (Donnelly and Woodruff, 2007).

A previous study from the Blue Hole, Belize found the sedimentary record from this site to be an excellent paleo-climate archive, representing one of the longest, undisturbed tropical cyclone archives in the Caribbean (Gischler et al., 2008). However, this previous study was focused on reconstructing paleo-climatic conditions (i.e., relative SSTs) using sedimentary and geochemical proxy techniques and not, as this study is, on reconstructing the site-specific paleo-hurricane record for the Blue Hole. Here we expand on the work by Gischler et al. (2008) and, as part of a collaborative effort to expand the spatial coverage of paleohurricane records throughout the Caribbean (Liu, 2004a), present the highest resolution record paleo-hurricane activity for the region to date. It is our hope that as newer and more well-constrained, high-resolution paleo-hurricane proxy records such as the one we present become available scientists may soon be able to confidently discern patterns that are consistent with known variations in paleo-atmospheric conditions.

3.2 Study Setting

Climate in the study area is subtropical with temperatures averaging 27°C in the summer months and 24°C in the winter months. During the dry summer months, the wind regime of coastal Belize is dominated by trade winds blowing from the E and NE and having an average speed of 5 – 7 m/s. These winds help to moderate temperatures on the atolls and along the coast and result in a mean wave approach direction throughout the barrier reef system from ~75° (ENE) (Gischler, 2003). The winter months are marked by a pronounced dry season accompanied by winds blowing from the N and NW. From June through November tropical storms and hurricanes move westward through the North Atlantic Basin and the Caribbean, these storms have repeatedly passed through the Belize Barrier Reef system throughout recorded history (NOAA, 2010).

The Blue Hole is located in the eastern lagoon of Lighthouse Reef, the smallest of the three isolated carbonate platforms offshore the Belize Barrier Reef System (Fig. 3.1). The feature is a cylindrical Pleistocene sinkhole (125 m deep, 320 m diameter) that formed as the result of the dissolution of a karstic cave roof (Dill, 1977). The Blue Hole is surrounded by a ring of nearly continuous coral patch reefs breeched by two passages, on the eastern and northern approaches (Fig. 3.2). Outside the ring of patch reefs, the lagoon floor is about 5 m deep, while inside a slope (approximately 30°) steepens to a vertical wall at about 10 m water depth (Gischler et al., 2008) (Fig. 3.3). The bottom one third of the water column within the Blue Hole is anoxic, as a pycno-/thermo-cline exists at approximately 90 m water depth (Dill, 1977). The flat bottom of the Blue Hole is blanketed by thick sediment derived from the biogenic carbonate sediment produced within the subtidal environment from Lighthouse Reef (Dill et al., 1998). Given that the deepest level of the lagoon floor surrounding the Blue Hole of Lighthouse Reef was flooded early in the Holocene (Gischler, 2003), the Holocene sediment package at the bottom of the Blue Hole is expected to cover about 7.8 ka, and up to 20 m of annually layered sediment (Gischler et al., 2008).

Having already been identified as being a potential hurricane archive (Gischler et al., 2008) the Blue Hole is a truly unique feature from which to reconstruct the paleo-

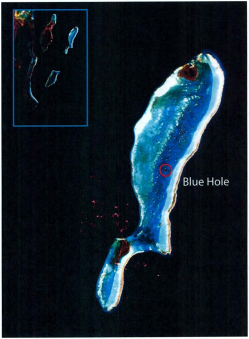

Fig. 3.1. Location map showing the position of the Blue Hole within the atoll system of the Belize Barrier Reef. http://www.nasa.gov/images/content/153203main_belize_hi.jpg

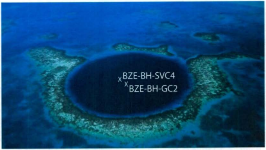

Fig. 3.2. Aerial photo of the Blue Hole looking east showing the locations of gravity (BZE-BH-GC2) and vibra (BZE-BH-SVC4) cores.

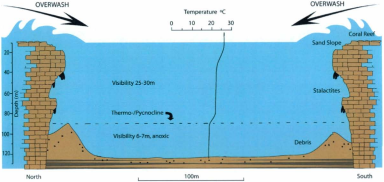

Fig. 3.3. Cross section of the Blue Hole, Belize (modified from Gischler, 2008).

hurricane record for storm-prone Belize. The "deep bucket" morphology and bottom-water anoxia of the Blue Hole make it unlikely that events potentially recorded in the sedimentary fabric are subject to post-depositional degradation by either physical or biological mixing. This means that unlike most paleotempestological sites where a minimum storm strength is required to create a preservable event (Bentley et al., 2002), the Blue Hole has the potential to be an archive for storms that may not have left detectable deposits elsewhere in the sedimentary record, thus providing the highest resolution proxy record of paleo-hurricane strikes available to date.

3.3 Methods

In June 2009, a Rossfelder vibracoring system was used to collect several long cores (to 6 m in length) from the bottom of the Blue Hole. Additionally, a simple gravity coring system was used to collect short cores (to 65 cm in length) from the same locations (Fig. 3.2). The cores were sent to Memorial University of Newfoundland where they were opened, and the sediment surface cleaned before being imaged using a high-resolution digital line scanning camera system integrated into a Geotek MSCL. Because whole-core MSCL data for cores across the Blue Hole displayed very similar stratigraphy, only one long core (BZE-BH-SVC2) and one short core, (BZE-BH-GC2) were described in detail and underwent further analysis.

Laminations and event sedimentation in both cores were observed manually and using a semi-automated method developed by the authors and described in detail in

Chapter 2. Sub-samples for grain-size analysis and $^{210}Pb/^{137}Cs$ radioisotope geochronology were taken at 0.5 cm intervals for the entire length of the gravity core (62.5 cm), while grain size was estimated visually along the length of the long vibracore. Samples were prepared for granulometric analysis by dispersing them in 0.05% sodium metaphosphate solution and subsequently disaggregating them in an ultrasonic bath. A Horriba LA-950 PARTICA particle size analyzer was then used to determine the grain-size distribution of the material. Activities of ^{210}Pb and ^{137}Cs were determined by γ-spectroscopy analysis of dried sediment (46.5 KeV peak for ^{210}Pb and 661 KeV peak for ^{137}Cs) (Cutshall et al., 1983). In addition, ten Accelerator Mass Spectrometry (AMS) ^{14}C ages from organic residue samples were obtained (Université Laval, QC, Canada and University of California, Irvine) along the length of the long core to help constrain the timing of events. Organic residue was separated from the sediment material by dissolving the carbonate with HCl, washing the sample with NaOH, and repeating until no carbonate material remained. These ages were calibrated using the Intcal09 and Marine09 (Reimer et al., 2009) curves and the OxCal (Ramsey, 2001, 2009) calibration program. Since no site-specific ΔR value is available for the Belize Atoll system, a global marine reservoir age of 405 y was used to calibrate the ^{14}C ages.

3.4 Results

3.4.1 Sedimentology

Normal background sedimentation in the Blue Hole consists of undisturbed/unbioturbated laminated biogenic carbonate mud (Fig. 3.4). These sediments are deposited in what have

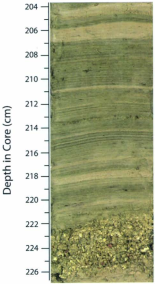

Fig. 3.4. Core BZE-BH-GC2. An example of a sediment surface from the Blue Hole, Lighthouse Reef, Belize. The sediment consists of alternating light (carbonate rich) and dark (organic matter rich) finely-laminated muds and silts that represent perennial background sedimentation. The colour variations represent seasonal alterations in organic matter within the water column. During the winter months the concentration of organic matter in the water column is greater that during the summer months due to seasonal upwelling. These fine laminations are interrupted by thicker coarse grained layers which are interpreted as event beds deposited by tropical storms and hurricanes in the area.

previously been described as annual couplets with the laminations resulting from seasonal changes in the organic matter content of the water column (Gischler et al., 2008). Individual laminae range in thickness from 1.0 to 1.5 mm, while total couplet thickness averages 2.3 mm (Figs. 3.4 and 3.5). Coarse-grained layers presumed to have been deposited as the result of more powerful sediment transport events (such as tropical cyclones) passing in the vicinity of the Blue Hole, are found interbedded with the perennial sedimentation (Fig. 3.4). These anomalous beds were differentiated from the background laminations on the basis of lithological and sedimentological characteristics including: sediment colour, bed thickness greater than that of annual couplets (unusually thick beds/ laminae > 2.5 mm) (Fig. 3.5), and grain-size coarser than that of normal background sediments (Fig. 3.6).

3.4.2 Geochronology and the Timing of Hurricane Strikes

A chronology established for the core material was determined using both the semi-automated counting of annual couplets and the AMS dating of organic matter found within the sediment column (Table 3.1). This chronology is presented in Figure 3.7 - a core log that includes AMS and annual couplet age data, and illustrates the major event layers observed within the sediment column. A comparison of the AMS determined sediment chronology shows an excellent correlation with sediment deposition determined by the counting of the annual couplets (Fig. 3.8), but yields an age offset of 339 y between the data sets. The ^{210}Pb profile is irregular, typical of non-steady state conditions (Nittrouer and Sternberg, 1981) (Fig. 3.6). The base of the excess $^{210}Pb_{XS}$ zone however, is below the maximum sampling depth of 62.5 cm and thus indicates that the entire

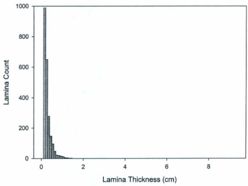

Fig. 3.5. Frequency distribution of lamina/bed thickness in sediment core material from the Blue Hole, Belize. The thickest beds (> 2cm) are not visible on this plot given their relative infrequency.

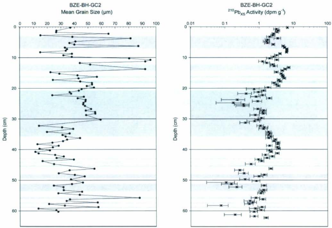

Fig. 3.6. Mean grain size (μm) and $^{210}Pb_{XS}$ profiles for the short gravity core BZE-BH-GC2. Highlighted intervals correspond to storm generated event beds visually identified in core material.

Table 3.1 Accelerator mass spectrometry (AMS) age data from organic residue in core materials from the Blue Hole, Belize (BZE-BH-SVC4). Ages are calibrated using a global marine reservoir age of 405 a, and have a 95% probability.

Depth (cm)	Thickness (cm)	Sample Lithology	Age Cal. yBP
27.9	0.5	Laminated biogenic carbonate mud	1555
67.0	0.5	Laminated biogenic carbonate mud	1420
140.6	0.7	Laminated biogenic carbonate mud	1275
175.3	0.6	Laminated biogenic carbonate mud	1205
222.4	1.0	Laminated biogenic carbonate mud	1110
260.9	1.0	Laminated biogenic carbonate mud	950
317.5	0.7	Laminated biogenic carbonate mud	910
362.4	1.0	Laminated biogenic carbonate mud	725
461.2	0.7	Laminated biogenic carbonate mud	580
516.9	0.9	Laminated biogenic carbonate mud	490

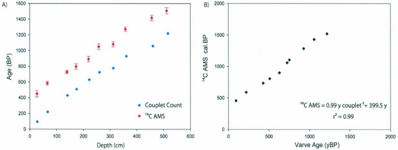

Fig. 3.7. A) Plot of Sediment Age (BP) vs. Depth in core (cm) as determined by calibrated ^{14}C AMS geochronology and by couplet counting. B) Plot of calibrated ^{14}C AMS Age (BP) vs. Varve Count Age.

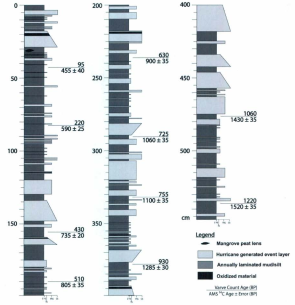

Fig. 3.8. Core log including ^{14}C AMS and varve count age data. Log is a composite of the short gravity core BZE-BH-GC2 and the long vibra-core BZE-BH-SVC4. Cores were correlated using a marker bed apparent at 20 cm depth.

gravity core is younger than ~110 y (roughly five half lives of ^{210}Pb). No excess ^{137}Cs was detected in the sediment core material (with a detection limit of 0.05 dpm g^{-1}).

3.5 Discussion

Based on the interpretation that coarse grained layers found interbedded with the perennial background sedimentation correspond to hurricane-generated event beds, the Blue Hole represents a uniquely well-preserved and continuous record of paleohurricane activity in the vicinity of the study area. The event beds are interpreted as having been deposited either by hurricane-generated overwash (Fig. 3.3) or by the storm wave base reached and activated sediment transport on the shallow lagoon floor inside the reef rimming the Blue Hole. Evidence supporting the redeposition of materials from the lagoon floor to the seabed has previously been presented by Gischler et al. (2008), wherein material dated using ^{14}C AMS techniques showed an age reversal.

Belize is located just north of the strike-slip zone between the Caribbean and North American plates, and as such tsunami surges triggered by major earthquakes could be preserved along with the hurricane record in the sediments of the Blue Hole. Unfortunately there are no widely applicable diagnostic criteria to distinguish storm (hurricane) generated event beds from tsunami-generated deposits in such a setting (Donnelly, 2005). The frequency of tsunamis near Belize however, is relatively low compared to the frequency of hurricane strikes, and as such the probability of a statistically significant number of suspected hurricane event layers actually representing tsunami strikes is low (McCloskey and Keller, 2009).

Although we are unable to directly determine sedimentation rates for the Blue Hole from $^{210}Pb_{XS}$ radioisotope geochronology data, we are able to establish a reliable chronology of events using a combination of calibrated ^{14}C AMS ages and ages determined by the counting of annually coupled laminae (Fig. 3.7). Although there is a 99% correlation between the two age models there is an apparent offset of ~339 y (Fig. 3.8). The consistency of the offset in ages between the two models, along with the presence of $^{210}Pb_{XS}$ which has a half-life of 22.3 years at 62.5 cm depth in gravity core BZE-BH-GC2 (Fig. 3.6) strongly suggests that this offset represents a "reservoir effect" – an older source of ^{14}C within the system that has yet to be accounted for and not a hiatus at the top of or within the sediment column.

The most recent event beds near the top of the core can be correlated to the historical record (Table 3.2) of hurricanes having passed within 100 km of the Blue Hole (NOAA, 2010). This search radius for comparison was chosen in an attempt to limit the number of storms considered to only those that would likely have had a significant impact on sediment mobilization and redeposition at the study area. Any discrepancies between the two records might be explained by the fact that some storms, while passing close by the Blue Hole, were relatively weak and incapable of depositing a sedimentary unit large enough to detect, or large enough to coat the bottom of the Blue Hole in its entirety. Earlier than the second half of the 20th century it becomes increasingly difficult to

Table 3.2. A comparison of hurricane-generated events detected in sediment material from the Blue Hole, to the historical record of storms passing within 100 km of the Blue Hole. It is important to note that the upper ~3.5 cm of core material is disturbed and no correlations are possible for this interval. Storms that passed within 100 km of the Blue Hole but did not leave a trace are believed to have been too weak to mobilize sediments capable of overwashing and blanketing the entire bottom of the Blue Hole.

Core Record Year (BZE-BH-GC2)	Corresponding Storm Name	Actual Year	Saffir-Simpson Category
1996	Mitch	1998	Tropical Storm
1992	Gert	1993	Tropical Depression
1987	—	—	—
Not Observed	Hermine	1980	Tropical Storm
1979	Greta	1978	Hurricane Cat. 3
Not Observed	Freida	1977	Tropical Depression
1973	Fifi	1974	Hurricane Cat. 2
Not Observed	Laura	1971	Tropical Depression
Not Observed	Edith	1971	Hurricane Cat. 1
1969	Francellia	1969	Hurricane Cat. 2
Not Observed	Unnamed	1964	Tropical Depression
1961	Hattie	1961	Hurricane Cat. 5
Not Observed	Gilda	1945	Hurricane Cat. 1
1943	Unnamed	1942	Hurricane Cat. 2
1940	Unnamed	1941	Hurricane Cat. 1

correlate event beds to known hurricane strikes. This is because the older historical record is largely considered to be unreliable, and often the only measure of hurricane strength comes from the major population center, Belize City which is located 70 km west of the study area on the leeward side of the Belize Barrier Reef system (McCloskey and Keller, 2009). We were however, able to establish a reliable chronology for these events using the techniques previously discussed.

The results show that while hurricanes have repeatedly affected the Blue Hole throughout the time period represented by the sediment column, the frequency of these strikes has not remained consistent. A frequency distribution diagram of hurricane-related deposits is presented in Figure 3.9 along with the 100-year return period for hurricane strikes. This-1200 year record shows that between ~ 600 and 1100 cal yBP, a time interval that corresponds to the Medieval Warm Period (MWP) (Lamb, 1965), the hurricane regime at the study site was significantly more active (100-y return period 4-7 y for detectable events) than the period preceding it (> 1100 yBP) as well as the period between ~ 500 - 100 cal yBP (return period 100-y return period 12 - 25 y) that corresponds to the timing of the Little Ice Age (LIA) (Matthes, 1939). The 20th century appears to be returning to a more active phase of hurricane activity (return period ~7 y for detectable events) (Fig. 3.9).

This study has produced a record of hurricane strikes on a shorter time scale but at much higher resolution than many other paleotempestological reconstructions, which for

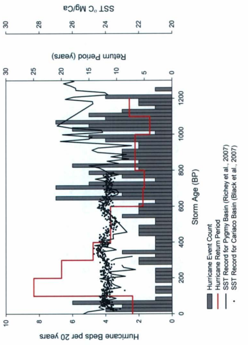
Hurricane Beds per 20 years
Storm Age (BP)
Return Period (years)
SST °C Mg/Ca
Hurricane Event Count
Hurricane Return Period
SST Record for Pygmy Basin (Richey et al., 2007)
SST Record for Cariaco Basin (Black et al., 2007)

the most part have recovered evidence of only major (> Category 3) hurricanes (Liu, 2004b). As a result, a direct comparison of paleo-hurricane strikes recorded in the sediment column from the Blue Hole to many of the existing paleotempestological records from sites located in the North Atlantic Basin is difficult. It is possible however, to compare the paleotempestological record from the Blue Hole to two independent estimates of basin-wide hurricane activity for the past 1500 years presented in Mann et al. (2009). The first estimate presented by Mann et al. (2009) is a compilation of sedimentary proxy reconstructions from five distinct regions; the Caribbean (Woodruff et al., 2008), the US Gulf Coast (Liu and Fearn, 2000), the southeastern US coast (Scott et al., 2003), the mid-Atlantic coast (Donnelly et al., 2004; Donnelly et al., 2001b; Scileppi and Donnelly, 2007), and New England (Boldt et al., 2010; Donnelly et al., 2001a) while the second estimate was obtained using a statistical model for Atlantic hurricane counts (Mann et al., 2007; Mann et al., 2009; Sabbatelli and Mann, 2007).

Like the paleotempestological record from the Blue Hole, both of these independent estimates show evidence for a peak in Atlantic hurricane activity during the MWP. Most interestingly perhaps is that our record, like the statistical model presented in Mann et al. (2009), shows that the peak activity levels during the MWP rival and even exceed modern hurricane activity levels. The statistical model attributes the MWP peak in activity to the reinforcing effects of La-Niña-like conditions and relatively warm Atlantic sea surface temperatures (SSTs) (Mann et al., 2009). The correlation between warmer Caribbean SSTs and peaks in hurricane activity and cooler SSTs and lulls in hurricane activity affecting the Blue Hole becomes obvious with the comparison of the paleotempestological record to high-resolution SST records from the nearby Cariaco and Pygmy Basins (Fig. 3.9), both of which show trends consistent with the SST record for the Blue Hole (Gischler et al., 2008). The decrease in hurricane activity also corresponds to a time when proxy records suggest a southerly displacement of the ITCZ (Haug et al., 2001) which is thought to have occurred as the result of colder polar temperatures (Hodell et al., 2005). It is thought that such a shift could potentially steer more tropical cyclones towards the southern Caribbean and away from the northern Caribbean and U.S. east coast (McCloskey, 2009).

3.6 Conclusions

Sediments from the Blue Hole contain a unique annually-resolved succession that records the paleohurricane record for Belize over the last ca. 1200 y. This record reveals centennial-scale variations in hurricane activity at the study area. A period of increased hurricane activity (return periods 4-7 y) is observed between ~600 and 1100 yBP, corresponding to the MWP during which SSTs in the Caribbean were relatively warm. A later period of decreased activity (return periods 12-25y) corresponds to the LIA, during which SSTs in the Caribbean were relatively cool, and the ITCZ is thought to have migrated south (Haug et al., 2001). The strong correlation between the timings of frequency shifts in landfalling hurricane activity observed at the Blue Hole and elsewhere in the Atlantic Basin (i.e., Mann et al., 2009) and known climatic variations strongly suggests that large-scale climatic events really are influencing hurricane activity levels. Given their potential to devastate coastal communities it is essential that we further our understanding of how large-scale climate phenomena affect the development and trajectory of hurricanes. An expansion of the paleotempestological data set for the Atlantic Basin, especially the development of more high-resolution proxy records such as the one presented here, and an increased number of reliable reconstructions of past large-scale climatic phenomena suspected of influencing hurricane activity will help scientists to do so.

References

Bentley, S.J., Keen, T.R., Blain, C.A., and Vaughan, W.C., 2002, The origin and preservation of a major hurricane event bed in the northern Gulf of Mexico: Hurricane Camille, 1969: Marine Geology, v. 186, p. 423-446.

BNMS, 2010, Belize National Meteorological Service Tropical Weather, Volume 2010: Belize City.

Boldt, K.V., Lane, P., Woodruff, J.D., and Donnelly, J.P., 2010, Calibrating a sedimentary record of overwash from Southeastern New England using modeled historic hurricane surges: Marine Geology, v. 275, p. 127-139.

Collins, E.S., Scott, D.B., and Gayes, P.T., 1999, Hurricane records on the South Carolina coast: Can they be detected in the sediment record?: Quaternary International, v. 56, p. 15-26.

Cutshall, N.H., Larsen, I.L., and Olsen, C.R., 1983, Direct Analysis of Pb-210 in Sediment Samples - Self-Absorption Corrections: Nuclear Instruments & Methods in Physics Research, v. 206, p. 309-312.

Dill, R.F., 1977, The blue holes, geologically significant submerged sinkholes and caves off Britisih Honduras and Andros, Bahama Islands: Proceedings of the 3rd International Coral Reef Symposium, v. 2, p. 237-242.

Dill, R.F., Land, L.S., Mack, L.E., and Schwarcz, H.P., 1998, A submerged stalactite from Belize: Petrography, geochemistry, and geochronology of massive marine cementation: Carbonates and Evaporites, v. 13, p. 189-197.

Donnelly, J.P., 2005, Evidence of past intense tropical cyclones from backbarrier salt pond sediments: A case study from Isla de Culebrita, Puerto Rico, USA: Journal of Coastal Research, p. 201-210.

Donnelly, J.P., Bryant, S.S., Butler, J., Dowling, J., Fan, L., Hausmann, N., Newby, P., Shuman, B., Stern, J., Westover, K., and Webb, T., 2001a, 700 yr sedimentary record of intense hurricane landfalls in southern New England: Geological Society of America Bulletin, v. 113, p. 714-727.

Donnelly, J.P., Butler, J., Roll, S., Wengren, M., and Webb, T., 2004, A backbarrier overwash record of intense storms from Brigantine, New Jersey: Marine Geology, v. 210, p. 107-121.

Donnelly, J.P., Roll, S., Wengren, M., Butler, J., Lederer, R., and Webb, T., 2001b, Sedimentary evidence of intense hurricane strikes from New Jersey: Geology, v. 29, p. 615-618.

Donnelly, J.P., and Webb, T., 2004, Back-barrier sedimentary records of intense hurricane landfalls in the Northeastern United Sates, *in* Murnane, R.a.L., K.B., ed., Hurricanes and Typhoons: Past, Present and Future: New York, Columbia University Press.

Donnelly, J.P., and Woodruff, J.D., 2007, Intense hurricane activity over the past 5,000 years controlled by El Nino and the West African monsoon: Nature, v. 447, p. 465-468.

Emery, K.O., 1969, A coastal pond studied by oceanographic methods: New York, Elsevier.

Fan, D.D., and Liu, K.B., 2008, Perspectives on the linkage between typhoon activity and global warming from recent research advances in paleotempestology: Chinese Science Bulletin, v. 53, p. 2907-2922.

Gischler, E., 2003, Holocene lagoonal development in the isolated carbonate platforms off Belize: Sedimentary Geology, v. 159, p. 113-132.

Gischler, E., Shinn, E.A., Oschmann, W., Fiebig, J., and Buster, N.A., 2008, A 1500-Year Holocene Caribbean Climate Archive from the Blue Hole, Lighthouse Reef, Belize: Journal of Coastal Research, v. 24, p. 1495-1505.

Haug, G.H., Hughen, K.A., Sigman, D.M., Peterson, L.C., and Rohl, U., 2001, Southward migration of the intertropical convergence zone through the Holocene: Science, v. 293, p. 1304-1308.

Hodell, D.A., Brenner, M., Curtis, J.H., Medina-Gonzalez, R., Can, E.I.C., Albornaz-Pat, A., and Guilderson, T.P., 2005, Climate change on the Yucatan Peninsula during the little ice age: Quaternary Research, v. 63, p. 109-121.

Lamb, H.H., 1965, The early Medieval warm epoch and its sequel: Palaeogeography Palaeoclimatology Palaeoecology, v. 1, p. 13-37.

Liu, K.B., 2004a, Paleotempestology of the Caribbean Region: A Multi-proxy, Multi-site Study of the Spatial and Temporal Variability of Caribbean Hurricane Activity, Inter-American Institute for Global Change Research.

—, 2004b, Paleotempestology: Principles, methods, and examples from Gulf Coast lake sediments, *in* Murnane, R., and Liu, K.B., eds., Hurricanes and Typhoons: Past, Present and Future: New York, Columbia Press, p. 464.

Liu, K.B., and Fearn, M.L., 1993, Lake-sediment record of late holocene hurricane activities from coastal Alabama: Geology, v. 21, p. 793-796.

—, 2000, Reconstruction of prehistoric landfall frequencies of catastrophic hurricanes in northwestern Florida from lake sediment records: Quaternary Research, v. 54, p. 238-245.

Madsen, A.T., Duller, G.A.T., Donnelly, J.P., Roberts, H.M., and Wintle, A.G., 2009, A chronology of hurricane landfalls at Little Sippewissett Marsh, Massachusetts, USA, using optical dating: Geomorphology, v. 109, p. 36-45.

Mann, M.E., Sabbatelli, T.A., and Neu, U., 2007, Evidence for a modest undercount bias in early historical Atlantic tropical cyclone counts: Geophysical Research Letters, v. 34, p. -.

Mann, M.E., Woodruff, J.D., Donnelly, J.P., and Zhang, Z.H., 2009, Atlantic hurricanes and climate over the past 1,500 years: Nature, v. 460, p. 880-U115.

Matthes, F.E., 1939, Report of the committee of glaciers: Transactions of the American Geophysical Union, v. XX, p. 518-523.

McCloskey, T.A., 2009, Proxy Records of Paleohurricanes for the Western and Southern Caribbean: Baton Rouge, Louisiana State University.

McCloskey, T.A., and Keller, G., 2009, 5000 year sedimentary record of hurricane strikes on the central coast of Belize: Quaternary International, v. 195, p. 53-68.

Murnane, R.J., and Liu, K.-b., 2004, Hurricanes and typhoons : past, present, and future: New York, Columbia University Press, 462 p.

Neumann, C.J., 1993, Tropical cyclones of the North Atlantic Ocean, 1871-1992: Asheville, N.C.

Nittrouer, C.A., and Sternberg, R.W., 1981, The Formation of Sedimentary Strata in an Allochthonous Shelf Environment - the Washington Continental-Shelf: Marine Geology, v. 42, p. 201-232.

NOAA, 2010, National Hurricane Center.

Ramsey, C.B., 2001, Development of the Radiocarbon calibration program OxCal: Radiocarbon, v. 43, p. 355-363.

—, 2009, Bayesian Analysis of Radiocarbon Dates: Radiocarbon, v. 51, p. 337-360.

Reimer, A., Baillie, M.G.L., Bard, E., Bayliss, A., Beck, J.W., Blackwell, P.G., Ramsey, C.B., Buck, C.E., Burr, G.S., Edwards, R.L., Friedrich, M., Grootes, P.M., Guilderson, T.P., Hajdas, I., Heaton, T.J., Hogg, A.G., Hughen, K.A., Kaiser, K.F., Kromer, B., McCormac, F.G., Manning, S.W., Reimer, R.W., Richards, D.A., Southon, J.R., Talamo, S., Turney, C.S.M., van der Plicht, J., and Weyhenmeye, C.E., 2009, Hadron-Initiated Emission Processes in Blazar Jets: International Journal of Modern Physics D, v. 18, p. 1511-1515.

Sabbatelli, T.A., and Mann, M.E., 2007, The influence of climate state variables on Atlantic Tropical Cyclone occurrence rates: Journal of Geophysical Research-Atmospheres, v. 112, p. -.

Scileppi, E., and Donnelly, J.P., 2007, Sedimentary evidence of hurricane strikes in western Long Island, New York: Geochemistry Geophysics Geosystems, v. 8.

Scott, D.B., Collins, E.S., Gayes, P.T., and Wright, E., 2003, Records of prehistoric hurricanes on the South Carolina coast based on micropaleontological and sedimentological evidence, with comparison to other Atlantic Coast records: Geological Society of America Bulletin, v. 115, p. 1027-1039.

Woodruff, J.D., Donnelly, J.P., Mohrig, D., and Geyer, W.R., 2008, Reconstructing relative flooding intensities responsible for hurricane-induced deposits from Laguna Playa Grande, Vieques, Puerto Rico: Geology, v. 36, p. 391-394.

CHAPTER 4

HIGH-RESOLUTION PALEO-HURRICANE RECONSTRUCTIONS FROM THE BLUE HOLE, BELIZE: A UNIQUE CONTRIBUTION TO THE PALEOTEMPESTOLOGICAL RECORD OF THE CARIBBEAN

4.1 Introduction

The primary objective of this thesis is to examine the paleotempestological record from sediment cores from the Blue Hole, Belize, as part of a collaborative effort to expand the paleotempestological coverage of the Caribbean. In order to facilitate the examination of this record, a simple tool was developed to semi-automate the detection and measurement of hurricane-generated event beds and the counting of fine, poorly developed laminae from the undisturbed core materials recovered from the Blue Hole. The results of this thesis project constitute an important contribution to the paleotempestological record of the Caribbean, providing the highest resolution record of paleo-hurricane strikes for this region to date. It is the hope of the author that these results will contribute to the broader understanding of paleohurricane activity and the associated forcing mechanisms at work in the Caribbean and the North Atlantic Basin.

4.2 Research Conclusions

4.2.1 Chapter 2 - The Development and Application of a Simple Tool for Lamina Recognition and Counting

Sediment cores collected from the Blue Hole contain a highly-resolved proxy record of hurricanes strikes. The high-resolution nature of this record results from background sedimentation in the Blue Hole consisting of finely laminated sediments deposited in what have previously been interpreted as annual couplets (Gischler et al., 2008). These laminations (~1 mm thick) are not always well developed or easy to define. A simple tool, presented as Chapter 2 of this thesis, was developed to overcome these obstacles and extract objective and reliable lamina thickness measurements and contact depths from high-resolution spatially-referenced digital images. This tool makes explicit use of the widely available Geoscan® line scanning camera system, Geotek ImageTools® software, and an easy to employ Matlab script. It provides users with a more objective lamina count than is possible through manual lamina counting (visual recognition) alone and allows users to identify event beds based on lamina/bed thickness, even at small scales. When an age model for the sediment core materials from the Blue Hole is constructed using a lamina count (material is deposited as annual couplets) performed by this new semi-automated tool is compared to an age model developed from ten calibrated ^{14}C AMS ages (Chapter 3) we see that there is a 99% correlation (Chapter 2) between the two. This extremely good correlation coefficient illustrates the usefulness and effectiveness of this tool in counting and measuring laminations in undisturbed core material.

4.2.2 Chapter 3 - A High-resolution Record of Hurricane Strikes from the Blue Hole, Belize: A Contribution to the Paleotempestological Record of the Caribbean.

The sediment-derived proxy record for hurricane strikes from the Blue Hole, Belize presented in Chapter 3 of this thesis, is the highest-resolution paleotempestological reconstruction for the Caribbean to date. These sediment core materials contain an annually-resolved record that has preserved evidence of hurricane strikes at this location for the past ca. 1200 years. This record reveals that hurricane activity in the vicinity of the Blue Hole has not been constant over the time but instead that hurricane activities have fluctuated over a multi-centennial timescale. Periods of increased hurricane activity are observed between ~600 and 1100 yBP, and 100 yBP to present and a period of decreased hurricane activity is observed between ~500 and 1000 yBP. The different activity regimes correspond to known climatic fluctuations including fluctuations in Caribbean and tropical Atlantic sea surface temperatures which warmed during the Medieval Warm Period (MWP) and cooled during the Little Ice Age (LIA) (Black et al., 2007; Richey et al., 2007) as well as to a known southerly displacement of the Inter-tropical Convergence Zone (ITCZ) which occurred at approximately the same time as the LIA (Haug et al., 2001).

4.3 Paleotempestology of the North Atlantic Basin: An Unresolved Debate

The importance of understanding large-scale variations in landfalling hurricane activities and the mechanisms responsible for them cannot be overstated (Knowles, 2008). The brevity of the historical prevents scientists from determining meaningful return periods for catastrophic hurricanes, which are among the costliest and deadliest of all landfalling storms, as so few have been recorded making landfall (Liu, 2007). The relatively short nature of the historical record also prevents us from being able to distinguish trends in hurricane frequency fluctuations on scales larger than inter-decadal. Sediment-derived hurricane proxy records have been established as reliable alternatives, providing scientists with the necessary tools to be able to reconstruct long-term changes in hurricane frequency patterns (Knowles, 2008).

The results presented in Chapter 3 of this thesis have revealed definitive multi-centennial fluctuations in hurricane landfall activities at the Blue Hole, Belize. These fluctuations correlate to and are likely influenced by documented large-scale climatic phenomena in the Atlantic Basin including changing SSTs associated with both the MWP and LIA (Black et al., 2007; Gischler et al., 2008; Richey et al., 2007) and the migration patterns of the ITCZ (Haug et al., 2001). The hypothesized connection between observed variations in landfalling hurricane activities in the Atlantic Basin and large-scale climate phenomena is strengthened when you compare the results presented in Chapter 3 to other paleotempestological records, namely the composite record produced by Mann et al. (2009) which shows the same peaks and lulls in basin-wide hurricane activity during the MWP and LIA, respectively. Understanding how large-scale climate phenomena have influenced past landfalling hurricane activities is the key to understanding how future hurricane activities will respond to our ever-changing climate. In order to accomplish this it is necessary that we expand and improve the quality of the paleotempestological data set for the Atlantic Basin by producing more high-resolution proxy records such as the one we presented in this thesis.

References

Black, D.E., Abahazi, M.A., Thunell, R.C., Kaplan, A., Tappa, E.J., and Peterson, L.C., 2007, An 8-century tropical Atlantic SST record from the Cariaco Basin: Baseline variability, twentieth-century warming, and Atlantic hurricane frequency: Paleoceanography, v. 22.

Gischler, E., Shinn, E.A., Oschmann, W., Fiebig, J., and Buster, N.A., 2008, A 1500-Year Holocene Caribbean Climate Archive from the Blue Hole, Lighthouse Reef, Belize: Journal of Coastal Research, v. 24, p. 1495-1505.

Haug, G.H., Hughen, K.A., Sigman, D.M., Peterson, L.C., and Rohl, U., 2001, Southward migration of the intertropical convergence zone through the Holocene: Science, v. 293, p. 1304-1308.

Knowles, J.T., 2008, A 5000 year history of Caribbean environmental change and hurricane activity reconstructed from coastal lake sediments of the West Indies: Baton Rouge, Louisiana State University.

Liu, K.B., 2007, Uncovering prehistoric hurricane activity - Examination of the geological record reveals some surprising long-term trends: American Scientist, v. 95, p. 126-133.

Richey, J.N., Poore, R.Z., Flower, B.P., and Quinn, T., 2007, 1400 yr multiproxy record of climate variability from the northern Gulf of Mexico: Geology, v. 35, p. 423-426.

Appendix A

Matlab Code

Explanation

Appendix A gives the code for the program used in Chapter 2 of this thesis – *inflection.m*. This code calculates the first differential from two inputs, depth and luminance values, both of which are extracted from high-resolution digital images using ImageTools software provided by Geotek. The zero-pass of the time-series for the first differential represents the depth of inflection points in the greyscale luminance curve, which is turn represent a change in colour in the sediment. Outputs from this program include the spatially referenced lamina/bed contact depths and lamina/bed thicknesses.

```
%%%%%%%%%%%%%%%%%%%%%%%%%%%%%%%%%%%%%%%%%%%%%%%%%%%%%%%%%%%%%%%%%%%%%%%%
% inflection.m
%
% This script takes two inputs, depth and luminescence. The inputs are
% taken as two columns in the array "data()"
% As this runs as a script (and not a function), all internal variables
% are published to the Matlab workspace for testing and troubleshooting
%
% Updated by David Shea, dshea@marport.com, Nov 29, 2010
%
% r1.0  Initial revision
% r1.1  Revised to add comments, and compare performance with built in
% matlab "diff" functions
% r1.2  Revised to calculate "non-zero inflection depths and
thicknesses"
% As per request by Dr. Sam Bentley.

% Input Parameters
% d     Vertical Depth in Core as Array (size n)
% l     Greyscale Luminescence          (size n)

% Output Parameters
% inflect   Inflection Points as Array (size n-2).
%           Column 1 (:,1) is inflection points (1 or 0)
%           Column 2 (:,2) is depth (meters)
%
%   How to use this function
%   >> inflect = inflection();
%
%   OR
%
%  >> inflect = inflection(d,l);
%%%%%%%%%%%%%%%%%%%%%%%%%%%%%%%%%%%%%%%%%%%%%%%%%%%%%%%%%%%%%%%%%%%%%%%%


function [inflect] = inflection(d,l)
if ~exist('d') || ~exist('l')
    warning('Depth or Luminescence not defined. Please enter filename');
    filename = input('Enter name of CSV file. Format must
be(depth,luminescence):','s');
    [d,l] = textread(filename,'%n,%n');
end

[x,d_size]=size(d);
[x,l_size]=size(l);
if (d_size ~= l_size)
```

```
    warning('Depth and Luminescence Array Sizes Do Not Match!');
    return;
end

%typically files are recorded as 0 to Max Depth. These lines reverse the
%arrays
%l = l(end:-1:1);
%d = d(end:-1:1);

[len,x]=size(d);
%---------------------------------------------------------------------
%calculate rate of change of luminescence relative to depth
%(1st derivative delta_luminescence / delta_depth
dl_dd = diff(l)./diff(d);

%All we care about is the sign of the 1st derivative
%this indicates +ve or -ve slope
signs=0;
signs = sign(dl_dd);

%setup our matrix for storing the inflection points
inflect=[0,0];

%finding inflection points, ie. sign changes in first derivative
for i=1:len-2 %must be len-2, because len(firstder) = len(depth) - 1
    if i==1
        if signs(i)~=signs(i+1);
            inflect=[1,d(i)];
        else
            inflect=[0,d(i)];
        end
    else
        if signs(i)~=signs(i+1);
            inflect=[inflect;1,d(i)];
        else
            inflect=[inflect;0,d(i)];
        end
    end
end

%inflectiondepths=[inflect,d(1:len-1)];
%---------------------------------------------------------------------

%diff_lum_diff_depth = diff(l)./diff(d);
%diff(diff_lum_diff_depth)
```

```
figure;
plot(dl_dd,d(1:end-1));
title('First Derivative of Luminescence vs. Depth');
xlabel('Luminescence');
ylabel('Depth (m)');

figure;
plot(inflect(:,1),inflect(:,2));
title('Inflection Points of Luminescence vs. Depth');
xlabel('Luminescence');
ylabel('Depth (m)');

bed_depths_index = find(inflect(:,1)); %find non-zero inflection points,
and output indices
bed_depths = inflect(bed_depths_index,2); %extract depths of non-zero
inflection points, using indices
bed_thickness = diff(bed_depths);
figure;
plot(bed_thickness(:),-bed_depths(1:(size(bed_depths)-1))); %create plot
of bed depth versus bed thickness
title('Bed Depth vs. Bed Thickness')
xlabel('Bed Thickness');
ylabel('Bed Depth (m)');
```

Appendix B

Extended Results of Grain-Size Analysis

Explanation

Appendix B contains the extended results of grain-size analysis preformed on sediment materials collected from the Blue Hole, Belize. Table B.1 lists the mean grain-size and percent fractions less than 2 μm, 4 μm, and 15 μm for each 0.5 cm sample interval along the core. Grain-size analysis was performed by dispersing sample material in a 0.05% sodium metaphosphate solution and subsequently disaggregating them in an ultrasonic bath. A Horriba LA-950 PARTICA particle size analyzer was then used to determine the particle-size distribution of the material.

Table B.1. Mean grain size values (μm) and percent fractions less than 2, 4, and 15 μm for sediment core materials from the short gravity core BZE-BH-GC2.

Depth Interval (cm)	*Mean Grain Size (μm)*	*% < 2 μm*	*% < 4 μm*	*% < 15 μm*
0 - 0.5	-	-	-	-
0.5 - 1.0	-	-	-	-
1.0 - 1.5	-	-	-	-
1.5 - 2.0	36.97	12.31	14.89	52.18
2.0 - 2.5	114.96	6.34	7.66	31.80
2.5 - 3.0	26.76	5.52	8.12	57.88
3.0 - 3.5	26.55	5.71	6.97	57.76
3.5 - 4.0	65.22	34.34	37.24	55.49
4.0 - 4.5	15.01	32.36	35.88	67.81
4.5 - 5.0	38.48	0.00	0.65	44.15
5.0 - 5.5	81.30	0.00	7.43	57.20
5.5 - 6.0	270.33	3.40	4.60	40.06
6.0 - 6.5	40.72	28.77	30.58	52.87
6.5 -7.0	36.29	11.79	13.19	39.37
7.0 - 7.5	39.92	6.81	8.64	40.25
7.5 - 8.0	86.97	10.18	12.43	42.51
8.0 - 8.5	32.98	10.35	12.55	51.14
8.5 - 9.0	34.56	5.81	7.80	44.22
9.0 - 9.5	33.60	26.59	29.32	47.76
9.5 - 10.0	14.80	35.96	38.91	72.62
10.0 - 10.5	38.11	31.36	33.50	47.83
10.5 - 11.0	31.84	30.01	31.53	47.60
11.0 - 11.5	38.02	7.71	9.31	58.96
11.5 - 12.0	80.27	21.93	24.03	36.51
12.0 - 12.5	95.76	21.87	23.24	33.34
12.5 - 13.0	91.97	5.30	6.39	32.83
13.0 - 13.5	43.91	18.93	20.63	46.39
13.5 - 14.0	51.57	13.77	14.93	31.23
14.0 - 14.5	134.54	9.34	10.24	25.33
14.5 - 15.0	100.77	0.01	7.11	24.41
15.0 - 15.5	91.91	0.01	10.35	28.94
15.5 - 16.0	-	-	-	-
16.0 - 16.5	22.26	17.02	18.61	41.71
16.5 - 17.0	28.88	11.64	13.30	40.69
17.0 - 17.5	42.18	0.00	0.13	33.88
17.5 - 18.0	56.59	4.70	6.38	31.42

Depth Interval (cm)	***Mean Grain Size (μm)***	***% < 2 μm***	***% < 4 μm***	***% < 15 μm***
18.0 - 18.5	42.95	10.69	12.03	31.49
19.5 - 20.0	52.84	0.12	1.63	19.88
20.0 - 20.5	52.95	0.32	2.41	22.27
20.5 - 21.0	49.00	7.60	8.41	22.79
21.0 - 21.5	54.39	3.44	4.58	13.27
21.5 - 22.0	45.17	0.00	0.46	30.97
22.0 - 22.5	43.11	10.87	11.78	27.14
22.5 - 23.0	36.42	16.24	17.15	28.39
23.0 - 23.5	37.49	14.84	15.83	30.04
23.5 - 24.0	-	-	-	-
24.0 - 24.5	46.83	11.56	12.26	21.18
24.5 - 25.0	42.27	14.77	15.37	24.77
25.0 - 25.5	48.16	0.00	0.00	28.31
25.5 - 26.0	47.96	0.00	0.00	27.32
26.0 - 26.5	46.48	0.01	1.53	27.93
26.5 - 27.0	46.31	0.00	0.69	24.04
27.0 - 27.5	47.63	0.00	0.00	23.95
27.5 - 28.0	51.91	0.00	0.18	24.05
28.0 - 28.5	52.18	0.00	0.11	24.57
28.5 - 29.0	48.24	6.75	8.24	27.20
29.0 - 29.5	55.20	0.00	0.00	20.27
29.5 - 30.0	55.34	0.00	0.00	19.22
30.0 - 30.5	48.49	0.00	0.00	26.81
30.5 - 31.0	47.16	5.41	7.40	32.04
31.0 - 31.5	188.90	0.85	2.41	19.15
31.5 - 32.0	59.20	0.00	0.00	20.48
32.0 - 32.5	1192.42	0.00	0.00	1.26
32.5 - 33.0	155.81	11.11	13.85	36.68
33.0 - 33.5	-	-	-	-
33.5 - 34.0	13.76	10.65	14.07	84.89
34.0 - 34.5	30.74	19.58	21.38	44.15
34.5 - 35.0	38.92	6.18	8.07	40.11
35.0 - 35.5	27.63	9.40	11.25	47.71
35.5 - 36.0	19.65	18.48	21.63	63.81
36.0 - 36.5	36.27	12.80	14.60	40.56
36.5 - 37.0	31.05	22.82	25.27	50.25
37.0 - 37.5	33.35	10.61	12.04	35.25
37.5 - 38.0	43.94	0.00	0.28	24.80

Depth Interval (cm)	***Mean Grain Size (μm)***	***% < 2 μm***	***% < 4 μm***	***% < 15 μm***
39.5 - 40.0	12.55	31.36	37.06	81.83
40.0 - 40.5	28.18	14.65	16.25	41.43
40.5 - 41.0	23.87	21.18	22.65	45.65
41.0 - 41.5	14.11	7.67	9.38	54.08
41.5 - 42.0	21.74	16.81	18.67	39.92
42.0 - 42.5	11.07	33.20	36.20	58.34
42.5 - 43.0	13.42	17.73	19.82	56.54
43.0 - 43.5	25.56	0.00	0.43	29.90
43.5 - 44.0	31.92	4.10	5.39	28.31
44.0 - 44.5	26.60	0.00	0.15	28.32
44.5 - 45.0	39.32	1.36	3.07	22.92
45.0 - 45.5	16.34	9.29	10.56	47.88
45.5 - 46.0	37.43	4.44	5.59	25.07
46.0 - 46.5	24.72	28.91	30.25	41.15
46.5 - 47.0	35.35	29.32	30.85	47.42
47.0 - 47.5	89.49	1.10	3.05	22.74
47.5 - 48.0	54.55	0.01	1.30	25.07
48.0 - 48.5	36.17	23.97	26.18	43.81
48.5 - 49.0	16.94	38.76	41.37	64.38
49.0 - 49.5	28.14	10.98	12.61	50.79
49.5 - 50.0	39.97	14.40	15.78	34.24
50.0 - 50.5	47.23	0.00	0.82	21.33
50.5 - 51.0	37.58	12.20	13.20	27.41
51.0 - 51.5	37.15	7.93	8.95	31.94
51.5 - 52.0	194.17	2.04	3.49	18.39
52.0 - 52.5	45.92	0.00	0.14	22.83
52.5 - 53.0	37.86	1.24	3.42	28.94
53.0 - 53.5	24.54	21.01	22.37	41.75
53.5 - 54.0	31.60	13.91	15.36	36.34
54.0 - 54.5	21.32	19.91	21.70	53.29
54.5 - 55.0	31.81	11.24	12.48	36.92
55.0 - 55.5	45.32	11.51	12.98	37.20
55.5 - 56.0	27.83	15.69	17.46	42.62
56.0 - 56.5	43.58	12.03	13.58	37.92
56.5 - 57.0	35.15	11.96	13.19	34.76
57.0 - 57.5	87.63	14.16	15.36	35.81
57.5 - 58.0	36.40	12.75	13.87	32.88
59.0 - 59.5	20.99	26.21	27.39	47.67

Depth Interval (cm)	*Mean Grain Size (µm)*	*% < 2 µm*	*% < 4 µm*	*% < 15 µm*
59.5 - 60.0	32.57	12.55	13.95	34.86
60.0 - 60.5	57.43	16.33	18.12	42.98
60.5 - 61.0	13.16	33.02	36.46	68.79
61.0 - 61.5	26.30	13.72	15.21	39.72
61.5 - 62.0	27.75	15.12	16.38	39.97
62.0 - 62.5	39.28	17.36	18.54	36.58

Appendix C

Extended Results of $^{210}Pb_{XS}$ Geochronology

Explanation

Appendix C contains the extended results of $^{210}PB_{XS}$ analysis preformed on sediment materials collected from the Blue Hole, Belize. Table C.1 lists the total activity (^{210}Pb dpm g^{-1}), the excess activity ($^{210}Pb_{XS}$ dpm g-^{1}), and the excess errors (dmp g^{-1}) for each measured sample interval along the core. $^{210}Pb_{XS}$ activities were determined by γ spectrometry (46.5 KeV peak) with a 0.05 dpm g^{-1} detection limit. It is important to note that no ^{137}Cs was detected in these materials (detection limit 0.05 dpm g^{-1}).

Table C. 1. $^{210}Pb_{XS}$ data for short gravity core BZE-BH-GC2

Depth Interval (cm)	*²¹⁰Pb Total Activity dpm/g*	*²¹⁰Pb Excess Activity dpm/g*	*²¹⁰Pb Excess Error dpm/g*
0 - 0.5	7.603560168	6.952762097	0.360994727
0.5 - 1.0	4.523854721	3.646561304	0.554612207
1.0 - 1.5	4.500570907	3.918649005	0.521523425
1.5 - 2.0	4.209311994	3.645768507	0.411645355
2.0 - 2.5	3.606861871	2.799362524	0.281767611
2.5 - 3.0	3.413532964	2.775844369	0.37837843
3.0 - 3.5	3.446579388	2.320541313	0.376414878
3.5 - 4.0	4.329958269	3.970940811	0.770601371
4.0 - 4.5	2.491902269	1.88731356	0.271568616
4.5 - 5.0	2.432901993	1.852238511	0.345792906
5.0 - 5.5	2.549332245	1.909124629	0.294714594
5.5 - 6.0	3.221926677	2.684970458	0.276871391
6.0 - 6.5	5.994010016	5.439546143	0.468470003
6.5 -7.0	6.338821024	5.848595575	0.39073596
7.0 - 7.5	7.326707771	6.953842326	0.506807992
7.5 - 8.0	7.618284008	7.022202649	0.502116035
8.0 - 8.5	7.234213271	6.698099504	0.431352874
8.5 - 9.0	5.049052604	4.345168698	0.359434106
9.0 - 9.5	4.46926425	3.604735113	0.446842965
9.5 - 10.0	3.536262141	2.932593134	0.431799058
10.0 - 10.5	2.930204207	2.232999816	0.386335872
10.5 - 11.0	4.700839909	3.657045661	0.451085387
11.0 - 11.5	2.039498502	1.386587622	0.287187332
11.5 - 12.0	2.645584404	1.840788497	0.340784935
12.0 - 12.5	3.309493878	2.69277636	0.337381935
12.5 - 13.0	3.932806627	3.150268569	0.659689574
13.0 - 13.5	8.977555218	8.165582191	0.706519358
13.5 - 14.0	7.044550166	6.323139433	0.522465526
14.0 - 14.5	5.740107217	5.144797116	0.457830716
14.5 - 15.0	4.266355623	3.514579119	0.431322278
15.0 - 15.5	5.341379305	4.745397718	0.433769453
15.5 - 16.0	5.956411983	5.245661544	0.484693062
16.0 - 16.5	6.18018202	5.426509204	0.465834102
16.5 - 17.0	6.914623438	6.006056249	0.596105974
17.0 - 17.5	4.873873014	4.068315875	0.407363393

Depth Interval (cm)	^{210}Pb Total Activity dpm/g	^{210}Pb Excess Activity dpm/g	^{210}Pb Excess Error dpm/g
18.5 - 19.0	4.232540925	3.507237252	0.458888101
19.0 - 19.5	4.44329985	3.939287982	0.454095267
19.5 - 20.0	2.827475453	2.054943277	0.370154944
20.0 - 20.5	1.641908844	0.858160566	0.288603612
20.5 - 21.0	1.88374005	1.385779744	0.213118337
21.0 - 21.5	1.601848103	1.036188322	0.244208864
21.5 - 22.0	1.07482972	0.490649791	0.181724672
22.0 - 22.5	1.922218435	1.363985093	0.280704178
22.5 - 23.0	1.488036674	0.921779084	0.254344557
23.0 - 23.5	2.621284103	2.164543332	0.348088771
23.5 - 24.0	0.869671841	0.293287811	0.150123591
24.0 - 24.5	1.522105784	1.006699466	0.279139192
24.5 - 25.0	0.896124015	0.241643508	0.119372828
25.0 - 25.5	1.040271434	0.420287967	0.161479061
25.5 - 26.0	0.884599879	0.392792485	0.14871623
26.0 - 26.5	-	-	-
26.5 - 27.0	1.533414514	0.980454786	0.218457582
27.0 - 27.5	1.894080064	1.432915866	0.280397925
27.5 - 28.0	1.810270479	1.323973847	0.229087596
28.0 - 28.5	1.89259138	1.420672195	0.301269264
28.5 - 29.0	1.408553093	0.849157994	0.232103185
29.0 - 29.5	-	-	-
29.5 - 30.0	1.899382324	1.241172185	0.22184977
30.0 - 30.5	1.562606947	0.959863055	0.184925515
30.5 - 31.0	1.282010588	0.826395797	0.29492069
31.0 - 31.5	1.193955596	0.438822779	0.120798159
31.5 - 32.0	-	-	-
32.0 - 32.5	1.748403513	1.178509052	0.241284222
32.5 - 33.0	2.238088185	1.586225532	0.387804794
33.0 - 33.5	2.219051099	1.516157248	0.365772936
33.5 - 34.0	-	-	-
34.0 - 34.5	2.728818439	2.048356098	0.339474747
34.5 - 35.0	3.005607812	2.202946755	0.35550199
35.0 - 35.5	2.749108581	2.069315156	0.349282206
35.5 - 36.0	3.27560309	2.400838582	0.387436914
36.0 - 36.5	2.811454676	2.110417489	0.372403484
36.5 - 37.0	3.708932087	3.106978868	0.323192143

Depth Interval (cm)	^{210}Pb Total Activity dpm/g	^{210}Pb Excess Activity dpm/g	^{210}Pb Excess Error dpm/g
38.0 - 38.5	4.578395751	3.790507832	0.432398671
38.5- 39.0	3.328383689	2.257297374	0.368942715
39.0 - 39.5	4.777442818	3.799800896	0.491140932
39.5 - 40.0	4.810093301	3.991554816	0.431534528
40.0 - 40.5	2.99402871	2.179199598	0.324309602
40.5 - 41.0	3.155732276	2.278614195	0.254003055
41.0 - 41.5	4.708237765	3.724207641	0.437273345
41.5 - 42.0	2.585245644	1.676543332	0.289943376
42.0 - 42.5	3.706362679	2.697670877	0.401468763
42.5 - 43.0	2.790229792	1.866896907	0.3132356
43.0 - 43.5	2.192176967	1.074610996	0.200775422
43.5 - 44.0	2.437111823	1.290380654	0.196151885
44.0 - 44.5	-	-	-
44.5 - 45.0	1.778161862	0.695841845	0.182131815
45.0 - 45.5	1.475155991	0.359262569	0.150573283
45.5 - 46.0	-	-	-
46.0 - 46.5	4.653792333	2.458754503	0.270696421
46.5 - 47.0	1.745095121	0.381760037	0.079633251
47.0 - 47.5	-	-	-
47.5 - 48.0	1.661358553	0.460261779	0.113438657
48.0 - 48.5	2.601071188	1.559369094	0.266340241
48.5 - 49.0	2.412177882	1.186553678	0.289437966
49.0 - 49.5	-	-	-
49.5 - 50.0	1.457143909	0.460590783	0.117945677
50.0 - 50.5	1.920210392	0.953520093	0.213650518
50.5 - 51.0	1.074527848	0.185700882	0.078312558
51.0 - 51.5	1.113362291	0.213487828	0.073178054
51.5 - 52.0	2.700999261	1.501335115	0.233790794
52.0 - 52.5	1.032255283	0.268478463	0.090257807
52.5 - 53.0	-	-	-
53.0 - 53.5	2.771153561	1.549832689	0.306417303
53.5 - 54.0	2.753837105	1.401463247	0.253545211
54.0 - 54.5	2.729998233	1.29249665	0.219213274
54.5 - 55.0	-	-	-
55.0 - 55.5	-	-	-
55.5 - 56.0	2.17787318	0.961160193	0.22174266
56.0 - 56.5	2.58319464	1.433812325	0.259182663

Depth Interval (cm)	*^{210}Pb Total Activity dpm/g*	*^{210}Pb Excess Activity dpm/g*	*^{210}Pb Excess Error dpm/g*
57.5 - 58.0	1.864493966	0.6255629	0.141040374
58.0 - 58.5	1.645127918	0.181495994	0.045561753
58.5 - 59.0	2.953232564	1.438481167	0.28564126
59.0 - 59.5	2.539540755	0.997684443	0.253607822
59.5 - 60.0	2.800977653	1.358261306	0.267372808
60.0 - 60.5	2.291302065	0.844363723	0.169531468
60.5 - 61.0	-	-	-
61.0 - 61.5	1.683051197	0.329998968	0.09927671
61.5 - 62.0	2.241065828	0.869486135	0.184355382
62.0 - 62.5	2.933778304	1.709695489	0.224459607

Appendix D

Extended Results of ^{14}C AMS Geochronology

Explanation

Appendix D contains the extended results of ^{14}C AMS analysis preformed on sediment materials form the Blue Hole, Belize. Tables 4.1 and 4.2 list the results of ^{14}C AMS dating as received from the Université Laval, Quebec, Canada. Samples of residual organic matter were sent here for preparation prior to being sent to the University of California at Irvine for AMS analysis. Table 4.3 lists the sample interval and calibrated ages (95% confidence interval) of ^{14}C AMS samples. Samples were calibrated using the OxCal program calibrated with the Intcal09 and Marine09 curves. Since no local reservoir age (ΔR value) has been determined for the Belize Atoll system, a global marine reservoir age of 405a was used in for calibration of these ages.

Table D.1. ^{14}C AMS data for long vibracore BZE-BH-SVC2

UNIVERSITÉ LAVAL

Laboratoire de Radiochronologie
Radiochronology Laboratory
Centre d'études nordiques
Québec, QC Canada

KECK CARBON CYCLE AMS FACILITY
Earth System Science Dept.
UNIVERSITY OF CALIFORNIA, IRVINE, CA, USA

^{14}C Results

Kathryn Denommee, Memorial University **Oct. 13, 2010**

University of California #	Université Laval #	customer ID (sample type)	Pre Treatments	fraction modern	±	$D^{14}C$ (‰)	±	^{14}C age (BP)	±
UCIAMS-83495	ULA-1861	BZE-BH-SVC 4-1 (organic matter)	HCl-NaOH-HCl	0,9103	0,0020	-89,7	2,0	755	20
UCIAMS-83496	ULA-1862	BZE-BH-SVC 4-2 (organic matter)	HCl-NaOH-HCl	0,8909	0,0019	-109,1	1,9	930	20
UCIAMS-83498	ULA-1863	BZE-BH-SVC 4-3 (organic matter)	HCl-NaOH-HCl	0,8701	0,0019	-129,9	1,9	1120	20
UCIAMS-83499	ULA-1864	BZE-BH-SVC 4-4 (organic matter)	HCl-NaOH-HCl	0,8604	0,0019	-139,6	1,9	1210	20
UCIAMS-83500	ULA-1865	BZE-BH-SVC 4-5 (organic matter)	HCl-NaOH-HCl	0,8511	0,0021	-148,9	2,1	1295	20
UCIAMS-83501	ULA-1866	BZE-BH-SVC 4-6 (organic matter)	HCl-NaOH-HCl	0,8340	0,0019	-166,0	1,9	1460	20
UCIAMS-83506	ULA-1868	BZE-BH-SVC 4-8 (organic matter)	HCl-NaOH-HCl	0,8135	0,0018	-186,5	1,8	1660	20
UCIAMS-83507	ULA-1869	BZE-BH-SVC 4-9 (organic matter)	HCl-NaOH-HCl	0,7958	0,0017	-204,2	1,7	1835	20
UCIAMS-83508	ULA-1870	BZE-BH-SVC 4-10 (organic matter)	HCl-NaOH-HCl	0,7874	0,0017	-212,6	1,7	1920	20

Radiocarbon concentrations are given as fractions of the modern standard, $D^{14}C$, and conventional radiocarbon age, following the conventions of Stuiver and Polach (Radiocarbon, v. 19, p.355, 1977).
Les concentrations radiocarbones sont données comme fractions du standard moderne, $D^{14}C$, et l'âge radiocarbone conventionnel suit les conventions de Stuiver et Polach (Radiocarbon, v.19, p.355, 1977)

Sample preparation backgrounds have been subtracted, based on measurements of ^{14}C-free wood.
Des échantillons préparés (provenant de bois sans ^{14}C) mesurant le bruit de fond de l'appareil, ont été soustraits

All results have been corrected for isotopic fractionation according to the conventions of Stuiver and Polach (1977).

Table D.2. Additional ^{14}C AMS data for long vibracore BZE-BH-SVC2

UNIVERSITÉ LAVAL
Laboratoire de Radiochronologie
Radiochronology Laboratory
Centre d'études nordiques
Québec, QC Canada

KECK CARBON CYCLE AMS FACILITY
Earth System Science Dept.
UNIVERSITY OF CALIFORNIA, IRVINE, CA, USA

^{14}C Results

Kathryn Denommee, Memorial University **Nov. 2, 2010**

University of California #	Université Laval #	customer ID (sample type)	Pre Treatments	fraction modern	±	$D^{14}C$ (‰)	±	^{14}C age (BP)	±
UCIAMS-84609	ULA-1867	BZE-BH-SVC 4-7 (organic matter)	HCl-NaOH-HCl	0,8300	0,0018	-170,0	1,8	1495	20

Radiocarbon concentrations are given as fractions of the modern standard, $D^{14}C$, and conventional radiocarbon age, following the conventions of Stuiver and Polach (Radiocarbon, v. 19, p.355, 1977).
Les concentrations radiocarbones sont données comme fractions du standard moderne, $D^{14}C$, et l'âge radiocarbone conventionnel suit les conventions de Stuiver et Polach (Radiocarbon, v.19, p.355, 1977)

Sample preparation backgrounds have been subtracted, based on measurements of ^{14}C-free wood.
Des échantillons préparés (provenant de bois sans ^{14}C) mesurant le bruit de fond de l'appareil, ont été soustraits

All results have been corrected for isotopic fractionation according to the conventions of Stuiver and Polach (1977).
Tous les résultats ont été corrigés en fonction du fractionnement isotopique selon les conventions de Stuiver et Polach (1977).

Comment:
This sample reacted very strongly with HCl during pre-treatments, indicating the presence of carbonates, which were removed by these pre-treatments.

Table D.3. ^{14}C AMS data calibrated for a global marine reservoir age of 405a

Sample Depth (cm)	***Memorial University Sample ID***	***95.4%***		***Mean Age (cal. BP)***
		From	***To***	
27.9	BZE-BH-SVC 4-1 (organic matter)	1485	1635	1555
67.0	BZE-BH-SVC 4-2 (organic matter)	1350	1460	1420
140.6	BZE-BH-SVC 4-3 (organic matter)	1230	1315	1275
175.3	BZE-BH-SVC 4-4 (organic matter)	1135	1275	1205
222.4	BZE-BH-SVC 4-5 (organic matter)	1040	1180	1110
260.9	BZE-BH-SVC 4-6 (organic matter)	885	1020	950
317.5	BZE-BH-SVC 4-7 (organic matter)	825	990	910
362.4	BZE-BH-SVC 4-8 (organic matter)	670	785	725
461.2	BZE-BH-SVC 4-9 (organic matter)	495	655	580
516.9	BZE-BH-SVC 4-10 (organic matter)	415	565	490